Patrik Mehlsack, BSc

Lipid-defined diet application and its impact on *Drosophila melanogaster*

A lipidomics approach

MASTER'S THESIS

to achieve the university degree of
Master of Science

Master's degree programme:
Biochemistry and Molecular Biomedicine

submitted to
Graz University of Technology

Supervisors
Mag. Dr. rer. nat. Gerald N. Rechberger
Institute of Molecular Biosciences, University of Graz

Mag. Dr. rer. nat. Harald F. Hofbauer
Institute of Molecular Biosciences, University of Graz

Graz, October 2020

AFFIDAVIT

I declare that I have authored this thesis independently, that I have not used other than the declared sources/resources, and that I have explicitly indicated all material which has been quoted either literally or by content from the sources used. The text document uploaded to TUGRAZonline is identical to the present master's thesis.

Date, Signature

First and foremost, I want to thank my supervisors, Dr. Gerald N. Rechberger and Dr. Harald Hofbauer, for their support and guidance throughout this project. I am very grateful for our friendly conversations and our academic and personal exchange.

I'd also like to thank Prof. Ronald P. Kühnlein for the opportunity to carry out this project in his lab and for his support throughout the project. Furthermore, I would like to thank the rest of the Kühnlein team for their help with *Drosophila*-related questions.

Big thanks to my parents, Sonja and Edwin, and my family for supporting me throughout my personal and professional development. Thank you for always providing a warm welcome for my visits to Vorarlberg.

Thanks to my friends in Vorarlberg for frequently visiting me. The times we spent here in Graz and will continue to spend in Vorarlberg will always be invaluable to me.

I'd also like to thank all my friends here in Graz for the great times we had and hopefully will continue to have throughout our lifes.

Very special thanks to my wonderful and beloved girlfriend Jacqueline for always supporting me in all matters. Thank you for all your love and encouragement, which helped me stay focused and determined throughout my studies.

Table of contents

Abstract

Drosophila melanogaster is an important model organism used for studies in many different scientific fields, such as aging, type 2 diabetes and neurodegenerative disorders. *Drosophila* has highly conserved metabolic pathways, such as lipid metabolism and insulin signalling, which have been profoundly studied. Despite *Drosophila* being widely used as model organism, there is only a limited number of studies addressing the food requirements, especially in regards to the lipids. For my master's thesis, yeast foods with different lipid compositions and their effect on the composition of the *Drosophila* lipid profile were analysed. Furthermore, the faeces of yeast-fed *Drosophila* were analysed, which shall gain first insights into the metabolisation capabilities of the digestive enzymes present in the gut. The conducted studies show that lipid dietary constraint only has minor effects on the lipid profile of *Drosophila melanogaster*. *Drosophila* utilises dietary fatty acids to its needs, with an emphasis on membrane lipids, which require a specific scope of fatty acyl chain lengths and degree of unsaturation in order to sustain membrane homeostasis. While the lipid profile of the membrane lipids is fairly steady, the di- and triacylglycerol reservoirs are subject to considerable fluctuations, which likely serve as buffer to provide fatty acids for membrane homeostasis. The analysis of the *Drosophila* faeces suggests that digestive enzymes of *Drosophila* are ineffective in breaking down triacylglycerol species with long chain fatty acids and a high degree of unsaturation. Future studies with a focus on the substrate specificity of *Drosophila's* intestinal lipases and the functions of the gut microbiome are promising to shed more light on the metabolisation of dietary lipids in *Drosophila melanogaster*.

Kurzfassung

Drosophila melanogaster ist ein wichtiger Modellorganismus, der in unterschiedlichsten Wissenschaftsfeldern, beispielsweise bei der Erforschung des Alterns, Typ-2-Diabetes und neurodegenerativen Störungen Anwendung findet. *Drosophila* verfügt über hochkonservierte Stoffwechselwege, unter anderem im Lipidmetabolismus und der Insulin Signaltransduktion, welche weitreichend untersucht wurden. Trotz der Tatsache, dass *Drosophila* in der Forschung breite Anwendung findet, gibt es nur wenige Studien, die den Nahrungsbedarf behandeln, besonders in Bezug auf den Lipidbedarf. Für meine Masterarbeit wurden mehrere Hefefutter mit unterschiedlichen Lipidzusammensetzungen und deren Effekt auf die Zusammensetzung des *Drosophila*-Lipidprofils untersucht. Zusätzlich wurden die Fäzes hefegefütterter *Drosophila* untersucht, um einen ersten Einblick in die Metabolisierung von Nahrungslipiden durch die Verdauungsenzyme im Darm zu erhalten. Die Untersuchungen zeigen, dass die Zusammensetzung von Nahrungslipiden lediglich einen geringen Einfluss auf das Lipidprofil von *Drosophila melanogaster* hat. *Drosophila* nutzt über die Nahrung aufgenommene Fettsäuren entsprechend ihrer Bedürfnisse. Der Fokus liegt dabei auf den Membranlipiden, welche eine bestimmte Bandbreite an Fettsäuren bezüglich Kettenlänge und Sättigungsgrad erfordern, um die Homöostase der Zellmembranen aufrecht zu erhalten. Während das Lipidprofil der Membranlipide weitgehend gleich bleibt, sind die Mengen an Di- und Triacylglycerol beträchtlichen Schwankungen unterworfen, was darauf hindeutet, dass diese Speicherlipide als Puffer zur Aufrechterhaltung der Membranhomöostase dienen. Die Analyse der *Drosophila* Fäzes legt nahe, dass die Verdauungsenzyme Triacylglycerol-Spezies mit langkettigen und hoch ungesättigten Fettsäuren nur ineffektiv metabolisieren können. Zukünftige Studien mit Fokus auf die Substratspezifität der intestinalen Lipasen und auf die Funktion des Darm-Mikrobioms versprechen einen genaueren Einblick in die Metabolisierung von Nahrungslipiden in *Drosophila melanogaster*.

Table of abbreviations

ACC	Acetyl-CoA carboxylase
Akh	Adipokinetic hormone
Bmm	Brummer lipase
CDP	Cytidine diphosphate
CDP-DAG	Cytidine diphosphate diacylglycerol
CK	Choline kinase
CPT	Choline phosphotransferase
CT	CTP:phosphocholine cytidylyltransferase
CTP	Cytidine triphosphate
DAG	Diacylglycerol
DGAT	Diacylglycerol acyltransferase
DHAP	Dihydroxyacetone phosphate
EK	Ethanolamine kinase
EPT	Ethanolamine phosphotransferase
ESI	Electrospray ionisation
ET	CTP:phosphoethanolamine cytidylyltransferase
FASN	Fatty acid synthase
Foxo	Forkhead box subgroup O
G3P	Glycerol-3-phosphate
GPAT	Glycerol-3-phosphate acyltransferase
HPLC	High-performance liquid chromatography
Hsl	Hormone-sensitive lipase
IP_3	Inositol-1,4,5-trisphosphate
IS	Internal standard
JH	Juvenile hormone
LDA	Lipid Data Analyzer
LPA	Lysophosphatidic acid
LPAAT	Lysophosphatidic acid acyltransferase
MAG	Monoacylglycerol
MGAT	Monoacylglycerol acyltransferase
m/z	Mass-to-charge ratio
PA	Phosphatidic acid
PAP	Phosphatidic acid phosphatase
PC	Phosphatidylcholine
PE	Phosphatidylethanolamine
PEMT	Phosphatidylethanolamine methyltransferase
PG	Phosphatidylglycerol
PGP	Phosphatidylglycerol phosphate
PI	Phosphatidylinositol
PIP	Phosphatidylinositol phosphate
PIP_2	Phosphatidylinositol-4,5-bisphosphate
PL	Phospholipid
PS	Phosphatidylserine
PSD	Phosphatidylserine decarboxylase
PSS	Phosphatidylserine synthase
PUFA	Poly-unsaturated fatty acid
QKO	Quadruple knockout
qTOF MS	Quadrupole time of flight mass spectrometry
SE	Steryl ester
TAG	Triacylglycerol
UPLC	Ultra-performance liquid chromatography

Introduction

Drosophila melanogaster as a model organism

Drosophila melanogaster has been used as a model organism for over a century. *Drosophila* first became known to a broader audience around 1910 when Thomas Hunt Morgan used it to define the mendelian theory of inheritance more precisely by specifying that genes are of physical origin and are situated on chromosomes [1]. His discoveries earned him the Nobel Prize in 1933 [2]. Ever since, *Drosophila* has been the subject of numerous studies, with a total of 6 Nobel Prizes awarded to studies based on *Drosophila* research, amongst them the Nobel Prize for "the genetic control of early embryonic development" in 1995, discoveries in the field of "odorant receptors and the organization of the olfactory system" in 2004, "discoveries concerning the activation of innate immunity" in 2011 and most recent the "discoveries of molecular mechanisms controlling the circadian rhythm" in 2017 [2], [3]. *Drosophila* also had a great impact on the successful sequencing of the human genome, as it was used to demonstrate the practicality of the shot-gun approach, which was later applied in the human genome project [4]. Nowadays, *Drosophila* is used in many disease-related fields of research, like cancer research and research of neurobiological and infectious diseases [5]–[7].

Drosophila bears highly conserved metabolic and signalling pathways, rendering it well-suitable as a model organism. Furthermore, the development of *Drosophila* from fertilisation to the adult fly at 25°C only takes around 10 days [8]. There are four stages in the life cycle of *Drosophila*: egg, larva, pupa and fly. After fertilization and egg laying, it takes around one day for the embryo to develop inside the egg before hatching. The hatched larva eats and grows and after five days pupates and enters metamorphosis, which involves the degradation of large parts of the larval tissue. With a median lifespan of 60-80 days, *Drosophila* is also broadly used in the field of aging [8]. Moreover, *Drosophila* serves as model for developmental biology since most of the adult tissues, like the eyes, wings and legs, are developed from a group of cells, referred to as "imaginal discs" [9]. Other reasons for using *Drosophila* as a model organism are the cheap acquisition and maintenance costs [9], the high number of offspring (*Drosophila* females lay up to 100 eggs per day) [10], the many tools for genetic manipulation of *Drosophila*, like, for example, the *UAS-GAL4* system [11] and the availability of numerous fly stocks from excellent stock centres (www.vdrc.at; https://bdsc.indiana.eu). Furthermore, there are only few restrictions and concerns regarding ethical issues with the use of *Drosophila* for laboratory experiments [9].

Drosophila lipid metabolism

The following summary of the lipid metabolism of *Drosophila* describes known enzymatic reactions and pathways and is based on the review "Triacylglycerol Metabolism in *Drosophila melanogaster*" by Christoph Heier and Ronald P. Kühnlein [12].

Across the eukaryotic kingdom, the neutral lipid triacylglycerol (TAG) and the carbohydrate glycogen are the most important energy storage molecules. TAGs are the most concentrated form of energy storage, due to their carbon atoms being in a highly reduced state and their high weight to energy content ratio [12]. TAGs are stored in lipid droplets that serve as reservoirs providing fatty acids as energy supply or membrane lipid precursors upon demand [13], [14]. Storing excess sugar and fat in the form of TAGs in lipid droplets also protects the cells from gluco- and lipotoxic stress, respectively [14]–[16]. The TAG storage capacity has a great influence on the membrane lipid metabolism and is therefore tightly regulated. In *Drosophila*, the TAG storage is regulated through various pathways, including insulin, adipokinetic hormone (Akh), juvenile hormone (JH) and ecdysone signalling [12]. The insulin signalling pathway regulates growth, stress responses, aging, reproduction, and metabolism [12]. In brief, *Drosophila* expresses multiple insulin-like peptides that act on the same insulin receptor, leading to alterations in the expression of several key metabolic enzymes [17]. Ultimately, it decreases the expression of Forkhead box subgroup O (Foxo), a transcription factor [18]. Since Foxo promotes lipase expression and TAG breakdown [19], activation of the insulin/Foxo pathway leads to repression of lipolysis. The neuropeptide Akh is produced in the corpora cardiaca by neuroendocrine cells and released into the haemolymph. It binds to the G protein-coupled Akh receptor that is located on fat body cells. Activation of the Akh receptor triggers several responses, amongst them the highly important and well-described activation of phospholipase C, which catalyses the conversion of phosphatidylinositol-4,5-bisphosphate (PIP_2) to inositol-1,4,5-trisphosphate (IP_3) and diacylglycerol (DAG), causing a release of intracellular Ca^{2+} [20]. Elevated cytosolic Ca^{2+} concentrations lead to an increase in TAG catabolism through a currently unknown mechanism [21]. The term juvenile hormone (JH) describes a group of acyclic sesquiterpenoids produced by the corpora allata that regulate insect traits like development, reproduction and aging [22]. Studies suggest an influence of JH signalling in the regulation of the TAG metabolism [23], [24], which is shown through reduced TAG levels within flies lacking the corpora allata or the transcription factor Met, which is activated by JH, while treatment with the JH analog methoprene leads to an increase in TAG [24]. Ecdysteroids are polyhydroxylated steroid hormones synthesised from cholesterol in the prothoracic gland of *Drosophila* larvae [25]. They are involved in the regulation of the TAG metabolism throughout various developmental stages. Ecdysteroids are required for TAG accumulation in mature female flies [26], regulating lipid homeostasis during oogenesis [26], [27] and promoting TAG accumulation during metamorphosis [28]. Several organs are involved in lipid absorption as well as in storage and utilisation of TAGs. After ingestion, TAGs are hydrolysed by digestive lipases, such as Magro (*CG5932*), into free fatty acids, glycerol and/or acylglycerol intermediates (*e.g.* DAG) in the midgut lumen. Enterocytes absorb these metabolites and incorporate them into complex lipids [29]–[31]. Dietary fatty acids and glycerol are converted into DAG by the enterocytes. DAG is the major transport form of neutral lipids in the haemolymph of *Drosophila* [32]. Excess dietary

fatty acids are converted to TAG for storage in intracellular lipid droplets [31], [32]. Enterocytes of the midgut also convert acetyl-CoA pools derived from dietary carbohydrates into fatty acids, which are either incorporated into TAG for local energy storage or into DAG for energy transport in the form of lipoprotein complexes between tissues [32], [33]. Lipids are delivered to the brain, oocytes, oenocytes, imaginal discs and other tissues through the haemolymph [32], [34], [35]. Midgut-derived DAG is primarily directed to the fat body, which acts as the main energy storing tissue and has a high capacity for TAGs [29], [32], [35].

Lipolysis and lipogenesis in *Drosophila*

Fat body TAG reserves are mobilised upon demand in times of starvation and are enzymatically hydrolysed to obtain DAGs and fatty acids, a process termed lipolysis. The main TAG lipase in *Drosophila* is the Brummer (Bmm) lipase, the ortholog of the mammalian adipose triglyceride lipase (ATGL) [36]–[39]. Knockout of the *bmm* gene encoding the Brummer lipase leads to excessive TAG accumulation and reduced TAG breakdown upon starvation [38]. Akh signalling, representing glucagon-like signalling in insects, regulates another lipolytic system in *Drosophila*, however, the key lipases regulated by this system are currently uncharacterised [39]. Further breakdown of DAG might be catalysed by the enzyme hormone-sensitive lipase (Hsl) [40], which remains to be experimentally confirmed. *De novo* synthesis of fatty acids in *Drosophila* requires two enzymes. The enzyme acetyl-CoA carboxylase (*ACC*) builds malonyl-CoA from acetyl-CoA. The enzyme FA synthase (*FASN*) produces long-chain fatty acids by condensing malonyl-CoA units with acetyl-CoA [41], [42]. *ACC* and *FASN* mainly contribute to storage lipid synthesis in the fat body and midgut [32], [35]. In the midgut, *de novo* lipogenesis produces DAG, which is then exported to the haemolymph to transport fatty acids to other tissues [32]. In the fat body, storage lipids are produced through *de novo* lipogenesis [15], [35], [43]. *De novo* lipogenesis in the fat body and the midgut fulfils crucial functions in sustaining energy homeostasis [43]. For transport or storage, fatty acids need to be converted into complex lipids, which involves esterification to a glycerol backbone. There are two pathways for the synthesis of TAG. The glycerol-3-phosphate (G3P) pathway [44]–[46] and the MAG-O-acyltransferase (MGAT) pathway [45]. In the G3P pathway, the G3P-O-acyltransferase (GPAT) transfers a fatty acid from acyl-CoA to G3P, forming lysophosphatidic acid (LPA) [44]–[46]. A subsequent acyltransferase reaction converts LPA to phosphatidic acid (PA), catalysed by the enzyme LPA acyltransferase (LPAAT). The PA phosphatase (PAP) converts PA to DAG, which can then be transported through the haemolymph [32]. Alternatively, monoacylglycerol (MAG) derived from complex lipids can be acylated by MGAT to produce DAG, which determines the point where both pathways converge [45]. Through an acylation of DAG by the DAG-O-acyltransferase (DGAT), TAG is formed [46]–[48]. The most prominent DGAT in *Drosophila* is the Midway (Mdy) enzyme [49].

Membrane lipid metabolism

Several biochemical pathways compete with the synthesis of TAG. Phospholipid (PL) biosynthesis uses the same initial steps, however the pathway branches off at PA or DAG [32]. The general eukaryotic phospholipid biosynthesis is shown in Figure 1. As the study focuses on the phospholipids phosphatidylethanolamine (PE) and phosphatidylcholine (PC), the biosynthesis of these lipid classes will be described in greater detail. The biosynthetic pathways of other physiologically important phospholipids are shown in grey. PE and PC have similar pathways where their head groups are phosphorylated, bound to cytidine diphosphate (CDP) and then bound to DAG [50]. For PC, the enzyme choline kinase (CK) attaches a phosphate group to choline using adenosine triphosphate (ATP). The enzyme CTP:phosphocholine cytidylyltransferase (CT) attaches CDP to choline using cytidine triphosphate (CTP). Lastly, DAG is bound to choline in a reaction where a phosphate remains on the choline, forming PC. This reaction is catalysed by the enzyme choline phosphotransferase (CPT) [50, pp. 218–222]. For PE, the enzyme ethanolamine kinase (EK) attaches a phosphate group to ethanolamine using ATP. The enzyme CTP:phosphoethanolamine cytidylyltransferase (ET) attaches CDP to ethanolamine using CTP. Lastly, DAG is bound to ethanolamine in a reaction where a phosphate remains on the ethanolamine, forming PE. This reaction is catalysed by the enzyme ethanolamine phosphotransferase (EPT) [50, pp. 228–232]. PE can be converted to PC through the enzyme PE methyltransferase (PEMT) through three subsequent methylation reactions using S-adenosyl-L-methionine as methylation donor [50, p. 222].

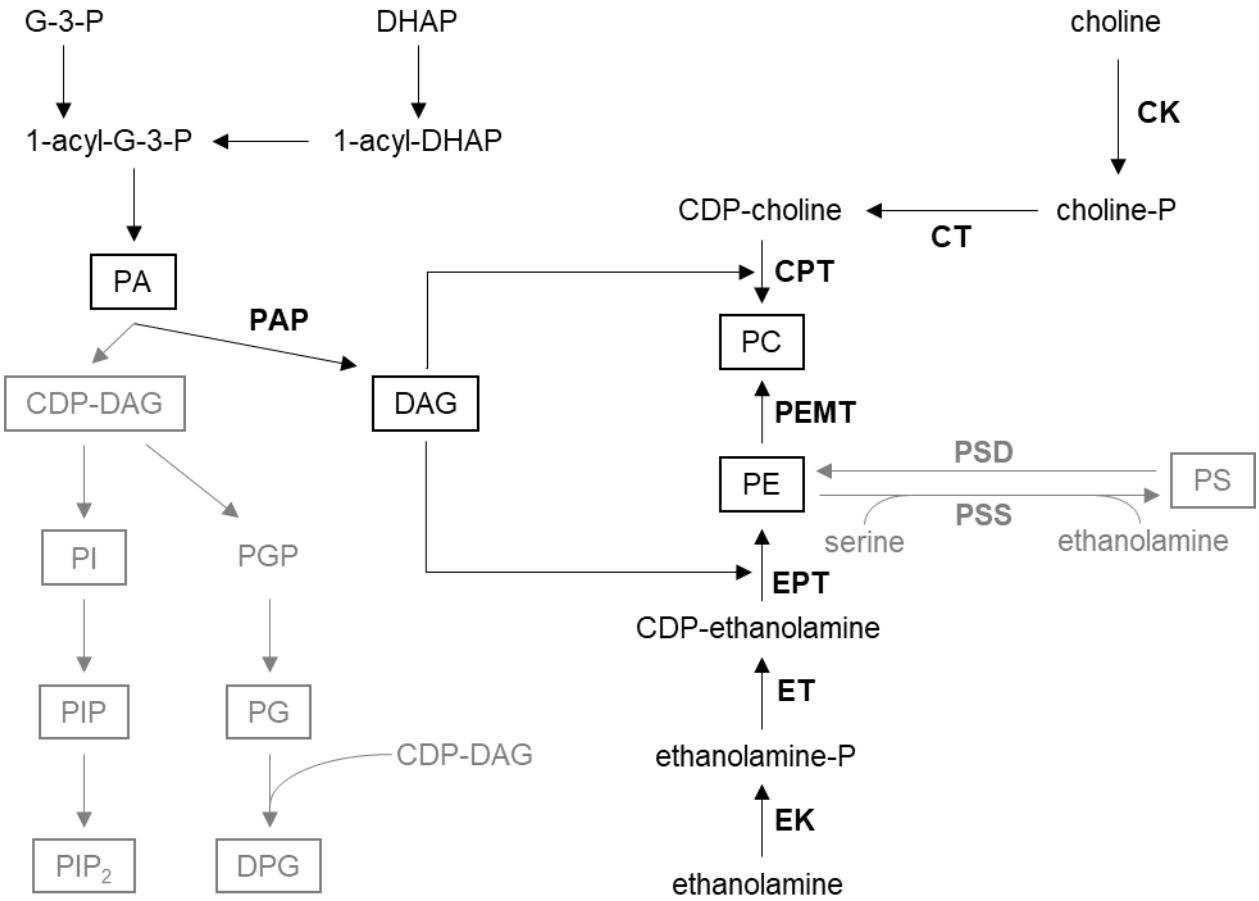

Figure 1: **Phospholipid biosynthetic pathways in eukaryotic cells.** Pathways that are relevant for this study are shown in black, others in grey. Abbreviations: G-3-P, glycerol-3-phosphate; DHAP, dihydroxyacetone phosphate; PA, phosphatidic acid; DAG, diacylglycerol; CDP-DAG, cytidine diphosphodiacylglycerol; PI, phosphatidylinositol; PIP, phosphatidylinositol phosphate; PIP_2, phosphatidylinositol 4,5-bisphosphate; PGP, phosphatidylglycerol phosphate; PG, phosphatidylglycerol; DPG, diphosphatidylglycerol; PAP, phosphatidic acid phosphatase; CK, choline kinase; CT, CTP:phosphocholine cytidylyltransferase; CPT, choline phosphotransferase; PC, phosphatidylcholine; EK, ethanolamine kinase; ET, CTP:phosphoethanolamine cytidylyltransferase; EPT, ethanolamine phosphotransferase; PE, phosphatidylethanolamine; PEMT, PE methyltransferase; PSS, phosphatidylserine synthase; PS, phosphatidylserine; PSD, phosphatidylserine decarboxylase. The pathways shown are taken from the textbook by D. Vance and J. Vance, “Biochemistry of Lipids, Lipoproteins and Membranes” [50, p. 215].

Food requirements of *Drosophila*

Like all other metazoans, *Drosophila* consumes and metabolises protein, carbohydrates and lipids. Due to the lack of synthetic defined standard food compositions, there is limited information available regarding specific food-derived lipid requirements of *Drosophila*. It is known that *Drosophila* is a sterol auxotroph. Sterols are required for the synthesis of the ecdysteroid hormones [51] and are important components to regulate biophysical properties of biological

membranes [52]. The standard food composition differs between laboratories, which ranges from simple foods like mashed bananas over sugar/yeast-based foods to complex foods containing yeast and plant ingredients. It is known that different foods (plant food, yeast food) have an effect on the *Drosophila* lipidome, since at low temperatures *Drosophila* resorts to plant food, which is high in lipid content and contains poly-unsaturated fatty acids (PUFAs), to ensure membrane fluidity during cold periods [31]. *Drosophila* is able to synthesise fatty acids from glucose or other dietary sugars [12], however, insufficient *de novo* PUFA production is described on food sources lacking PUFAs, indicating the absence of fatty acid desaturases other than delta-9 desaturases in its genome [53].

UPLC-qTOF mass spectrometry

Ultra-performance liquid chromatography (UPLC) is a chromatographic separation method that is based on the principle of high-performance liquid chromatography (HPLC), which has been used in laboratories for decades [54]. In HPLC, analytes, along with an eluent termed mobile phase, are pumped with high pressure through a separation column. The column contains a stationary phase, which interacts with analytes in the mobile phase. Depending on the material, the different analytes interact to a greater or lesser extent with the stationary phase. The stronger the interaction with the column material is, the longer it takes for a substance to pass the column. For the separation of lipids, a reverse phase chromatography column is used. Reverse phase columns have a hydrophobic stationary phase, which leads to a stronger retardation of more hydrophobic substances [55].

The most common ionisation technique in lipid mass spectrometry is the electrospray ionisation (ESI) [56]. The principle of ESI is that a solution containing the analyte is channelled through a metal capillary, to which a voltage is applied. An electric field emerges between the capillary and an opposing electrode, which prompts the solution to move electrophoretically towards the electrode. At the tip of the capillary, an excess of ions of the same charge state begin to repel each other, leading to the formation of a Taylor cone, where the particles leave the capillary as aerosol. An inert gas (*e.g.* nitrogen) promotes the evaporation of the solvent. The evaporation leads to a decrease of the droplet size until the droplet radius drops below the Rayleigh limit, where the droplets disintegrate due to the repulsion of the equal charges, which is referred to as Coloumb fission. There are different models describing the formation of free ions in the gaseous phase. The Charged Residue Model assumes that after subsequent Coloumb fissions, tiny droplets of 1 nm in diameter remain that contain only one analyte molecule each. The Ion Evaporation Model assumes that free ions are released from larger droplets into the gaseous phase. The resulting ions are channelled into the mass spectrometer as a result of the difference of potential between the spray capillary and the opposing electrode, which contains an orifice for the passage of the ions [57].

Quadrupole time of flight (qTOF) mass spectrometry uses a hybrid system composed of a quadrupole mass analyser and a time of flight mass analyser connected in a serial fashion. The quadrupole mass analyser works in principle as a mass filter that only allows ions with a specific mass-to-charge (m/z) ratio to pass through to the detector. It contains four rod-shaped metal electrodes arranged in a parallel fashion (quadrupole), which only allow passage of ions of a defined m/z ratio using a combined voltage field of direct and alternating current, where the ions of interest pass through on a stable, oscillating path. Other ions move on instable paths and ultimately collide with the metal rods [58, p. 354]. Time of flight mass spectrometers use a high vacuum system with a very precise measurement of the time between the start of the ions from the source to their arrival at the detector. The ions are accelerated through an electrostatic field to reach the same kinetic energy and travel a specified path, referred to as drift region, after leaving the source. Ions of different m/z ratios travel at different velocities, allowing detection of the m/z ratio of an ion through its time of flight [58, p. 327]. The combination of two mass spectrometry techniques allows for MS/MS experiments, therefore enabling more accurate identification of molecules. It combines the advantage of the quadrupole, which is the possibility of structural identification via fragmentation experiments, with the high mass accuracy of the time of flight analyser [58, pp. 327, 354].

Lipid analysis using UPLC-qTOF mass spectrometry

Lipids are mainly water-insoluble, hydrophobic molecules that can only be dissolved in organic solvents (*e.g.* chloroform, methanol). Depending on their moieties, lipids have different degrees of hydrophobicity. Neutral lipids and waxes are extremely hydrophobic, while phospholipids and glycolipids contain hydrophobic and hydrophilic moieties. Lipids serve as energy supply and storage and can act as signalling molecules. The main groups of lipids in the biological context are the neutral triacylglycerols (TAGs) that serve as energy storage and provide fatty acids as building blocks for other lipid classes and the phospholipids (PLs) like phosphatidylserine (PS), phosphatidylcholine (PC), phosphatidylethanolamine (PE), phosphatidylinositol (PI) and others, which serve as membrane lipids, forming a lipid-bilayer with their hydrophobic side chains directed to the inside. Other important lipid classes are the glycolipids, like the sphingolipids, and the sterols, which both occur in lipid-bilayers. TAGs are neutral, non-charged lipids that are composed of a glycerol backbone, to which 3 fatty acids are esterified. Due to them neither being charged nor containing any hydrophilic moieties, these are extremely hydrophobic substances. Phospholipids are composed of a glycerol backbone, to which 2 fatty acids and a hydrophilic phosphate-containing head group are esterified, making them much more hydrophilic compared to TAGs. Fatty acyl chains may contain one or more double bonds. These unsaturated fatty acids have lower melting points compared to their saturated counterparts, which leads to a more flexible membrane structure at low temperatures [59, pp. 50–51].

The challenging parts of lipid analysis are on the one hand the proper separation of lipids that behave entirely different in regards to polar and non-polar solvents and on the other hand the separation of lipids of the same class that only differ in as much as a double bond within the molecule. The methods used here are based on the method described by Knittelfelder et al. [56] The method uses a UPLC separation with a solvent gradient, ensuring proper separation of the polar phospholipids and the non-polar triacylglycerols within the same run using the same column. An advantage of UPLC-coupling is the pre-separation of different lipids that have the same mass to charge ratio. Mass spectrometry without prior chromatographic separation would make it impossible to distinguish between these molecules. The chromatographic separation enables the identification of the analysed lipids according to their retention time. The chromatographically separated lipids elute in the following order: lysophospholipids, phospholipids, diacylglycerols and sphingolipids (partly overlap with the phospholipids), triacylglycerols. After chromatographic separation, the lipids are ionised through electrospray ionisation. Most lipid classes produce several different ions, however there is usually a type of ionisation that works best for each class. For our study, we examined the $[M + NH_4]^+$ adducts for the TAGs, the $[M + H]^+$ adducts for the PCs and PEs and the $[M + Na]^+$ and $[M + H - H_2O]^+$ adducts for the DAGs. The different lipids are then analysed using qTOF mass spectrometry [56]. The exact procedure of peak detection, peak integration and data evaluation is described in the material and methods chapter.

Project outline

The aim of my master's thesis was to study the effect of yeast foods with different lipid compositions on the lipidome of *Drosophila melanogaster*. For the yeast foods, we used a wild type strain (*Saccharomyces cerevisiae*) as reference food, a mutant strain incapable of producing TAG (QKO; quadruple knockout) [60], [61] and a mutant strain that accumulates TAG and additionally produces longer fatty acids (*acc1**) [62] to visualise the impact of low, medium and high TAG-containing food on the lipidome of *Drosophila*. In addition, a commercial brewer's yeast, which is also component of the standard laboratory food, was used as further food source of yet unknown origin and lipid composition. Aside from wild type *Drosophila* flies (w^{1118}), we used mutant flies lacking the Brummer lipase (bmm^{1}), the main TAG lipase in *Drosophila* [38]. This shall give us an insight on how a fly with an impaired ability to mobilise storage TAG reacts and adapts its lipidome to different dietary constraints. Lastly, we wanted to analyse the lipid profile of the faeces of *Drosophila*, which shall give an overview on which lipids *Drosophila* is able to absorb and process and which are excreted, possibly revealing insights in the function and specificity of intestinal lipases of *Drosophila*. Figure 2 shows the graphical outline of the project.

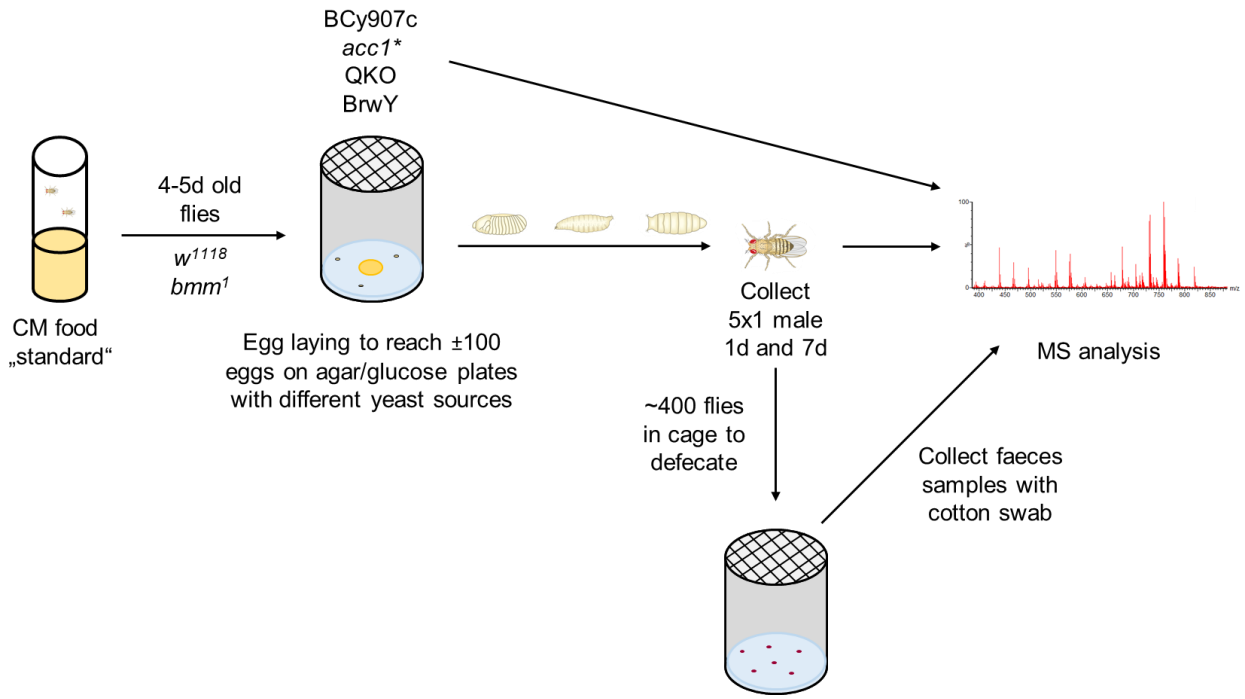

Figure 2: **Graphical outline of the master's thesis project.** 4-5 days old wild type and *bmm*^{1} flies laid approximately 100 eggs in fly cages containing the different food sources. The embryos went through the different developmental stages until they reached adulthood. 1 day and 7 days after eclosion, the lipids of 5 individual males from each of the different feeding conditions were extracted and analysed. Additionally, the different yeast food lipids were extracted and analysed and around 400 brewer's yeast-fed flies of both genotypes were put in a cage, where they were left to defecate for 24 hours. The faeces were collected and their lipids were extracted and analysed. (The *Drosophila* images used here were taken from the Memorial University of Newfoundland [63].)

Results

Quality control

In order to check the quality of the lipid extracts and the UPLC-qTOF setup, we performed several quality control measurements. Amongst them we analysed the following 5 blanks (Figure 3). The first blank contains only solvent without any further processing. The other four blanks were treated like samples for lipid extractions (see *Material and methods* section) but without any sample content. They initially contained i) only solvent ("Solvent extraction"), ii) solvent and a metal bead ("Solvent + metal bead extraction"), iii) solvent and internal standard ("Solvent + IS extraction") and iv) solvent, a metal bead and internal standard ("Solvent + IS + metal bead extraction"), respectively, prior to the lipid extraction procedure. The internal standards are marked with a red asterisk (*). The standard PE 34:0 (RT 10.04 min) is not seen, as it is masked by the peak of the standard PC 34:0 (RT 9.93 min). The peaks at 1.62 min and 10.85 min are known peaks that arise from the solvents. The solvent extraction shows a peak at 6.52 min, however the combination of the m/z found (m/z 338.3499) and this specific retention time exclude this substance from being a relevant lipid molecule and thus from any further interest in this study.

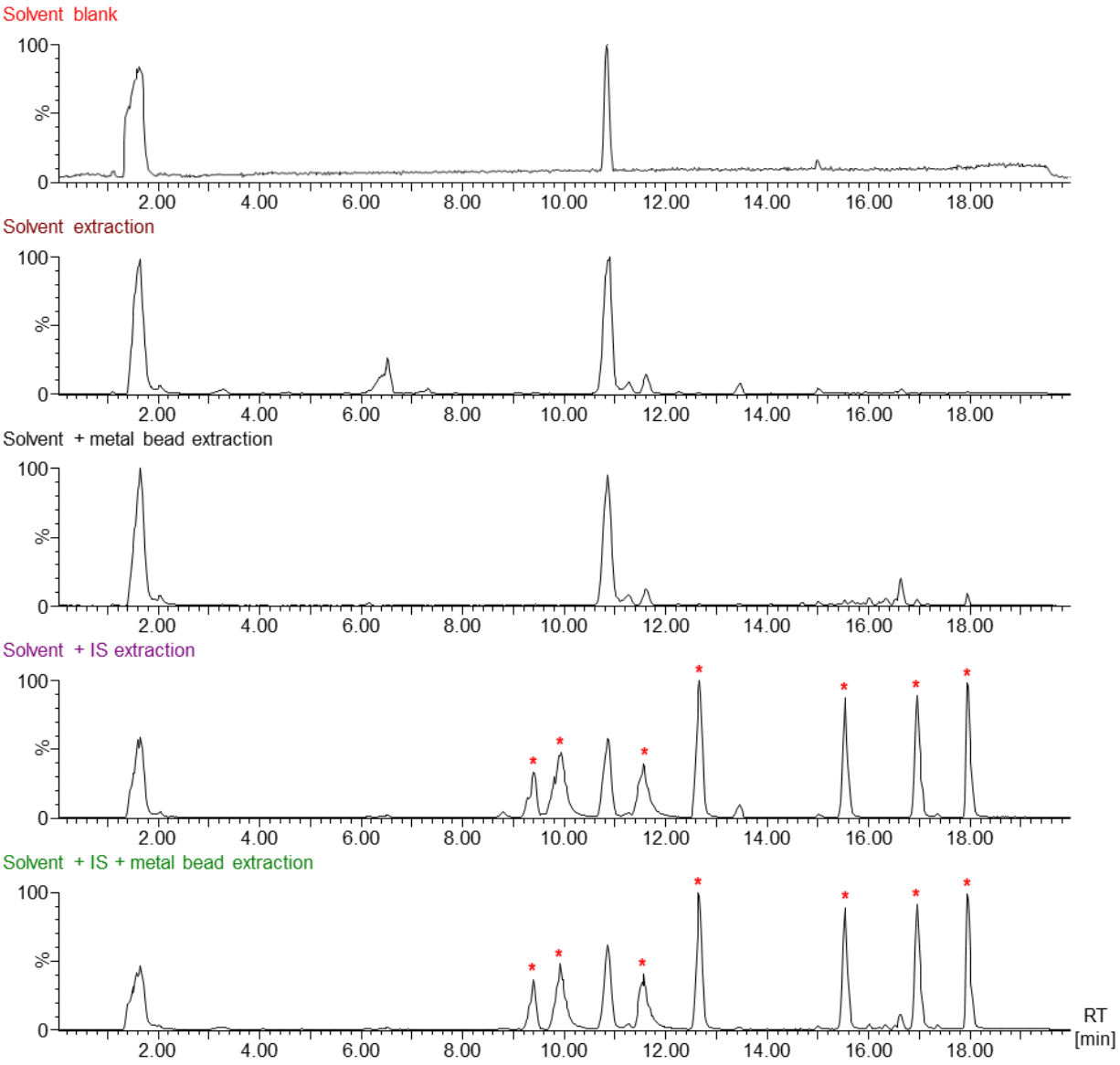

Figure 3: **Chromatograms of a solvent blank and 4 blank extractions.** "Solvent blank" is composed of only solvent (100 µl isopropanol, 50 µl chloroform/methanol (2/1, v/v)) injected into the MS. The other blanks were treated like lipid extraction samples. "Solvent extraction" is solvent only, "Solvent + metal bead extraction" is solvent extracted with a metal bead, "Solvent + IS extraction" is solvent and internal standard and "Solvent + IS + metal bead" is solvent and internal standard that was extracted with a metal bead. The internal standards are marked with a red asterisk (*) and are as follows: DAG 28:0 (RT 9.39 min), PC 34:0 (RT 9.93 min), PC 38:0 (RT 11.57 min), TAG 36:0 (RT 12.67 min), TAG 45:0 (RT 15.53 min), TAG 51:0 (RT 16.95 min), TAG 57:0 (RT 17.95 min). The standard PE 34:0 (RT 10.04 min) is not visible on the chromatogram, as it is masked by the peak of the standard PC 34:0.

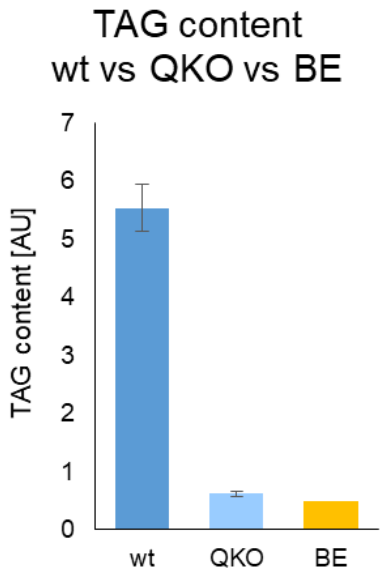

The software “Lipid Data Analyzer” (LDA) found TAG peaks for blank extractions and the quadruple mutant, both of which are not supposed to contain any TAGs. Figure 4 shows a comparison of the TAG content of the wild type yeast, the QKO mutant and a blank extraction (BE). The Figure shows that the amount of TAG found in the quadruple mutant is essentially the same amount that is found in a blank run.

Figure 4: **Comparison of the TAG content of the wild type yeast, the QKO mutant and a blank extraction**. The content is displayed in arbitrary units. (n=3 for wt and QKO)

Lipid analysis of different yeast food sources

Figure 5 shows the total TAG, PE, PC and DAG contents of the different yeast foods used in the experiments, as well as the distribution of acyl chain lengths and degree of unsaturation within these lipid classes. As seen in Figure 5A, the hyperactive *acc1** mutant had around twice the amount of TAG compared to the wild type strain and the brewer’s yeast, which both had similar TAG contents. The QKO mutant is described to be genetically unable to produce TAGs [60], [61]. The TAG amounts that were detected in the QKO mutant were similar to the TAG content found in blank extractions and thus only represent background noise (Figure 4). All the yeasts showed similar amounts of PE with slightly lower amounts for the QKO and *acc1** mutants. For the PC content, the wild type and *acc1** strains showed similar amounts, while the PC content for the QKO mutant was only around half the amount. The brewer’s yeast had a higher amount of PC compared to the other yeasts. The DAG content was essentially the same for all the different yeast foods. Figure 5B shows the TAG acyl chain lengths and degree of unsaturation of the yeast foods. The *acc1** mutant is described to produce longer acyl chains compared to the wild type strain, with a similar degree of unsaturation [64]. The brewer’s yeast had a wide distribution of TAG acyl chain lengths with a much higher amount of short TAG species (40:X to 44:X) and also contained a much higher amount of saturated TAGs (X:0) compared to the other yeasts. Moreover, the brewer’s yeast was the only one containing fatty acids with more than one double bond, as shown by the presence of TAG molecules with four to six double bonds (X:4 to X:6) and PCs and PEs with three double bonds (X:3), which were not present in the other yeasts, as *S. cerevisiae* yeast strains (wt, *acc1*,* QKO) are unable to produce fatty acids with more than one double bond [65]. Figure 5C shows a similar distribution of PE acyl chain lengths for the wild type yeast, QKO mutant and the brewer’s yeast. The *acc1** mutant showed a shift in PE composition towards species with longer acyl chain length (34:X and 36:X) and a concomitant reduction in

32:X species. The degree of unsaturation in PE was similar for all the *S. cerevisiae* strains and slightly more saturated in the brewer's yeast. Figure 5D shows the distribution of PC acyl chain lengths and degree of unsaturation. As for the PEs, the PC acyl chain lengths distribution of the wild type and QKO strains was similar, while the brewer's yeast contained a large proportion of shorter PC molecules, whereas the *acc1** strain shifted the profile towards longer acyl chains. The degree of unsaturation was similar for the wild type, the QKO and *acc1** strains. The distribution of DAG acyl chain lengths, seen in Figure 5E, was similar to the distribution of the PCs. The wild type yeast and the QKO mutant had a similar distribution with 34:X being the most abundant DAG acyl chain length. The *acc1** mutant had on average longer DAG acyl chains with 36:X as the most abundant DAG acyl chain length. The brewer's yeast additionally contained short DAG species (24:X to 28:X). The degree of unsaturation was similar for the *S. cerevisiae* strains (wt, *acc1*,* QKO). The brewer's yeast contained considerable amounts of saturated DAGs, which was also observed for the PCs.

In conclusion, these data prove the unique properties of the well-characterised *S. cerevisiae* strains with regard to their TAG content, acyl chain composition and degree of unsaturation, qualifying them as a powerful tool for the subsequent feeding studies to potentially modulate the lipidome of *Drosophila*. Moreover, the lipid profile of the commercial brewer's yeast was characterised and revealed very different properties with regard to lipid acyl chain composition and degree of unsaturation compared to the *S. cerevisiae* strains.

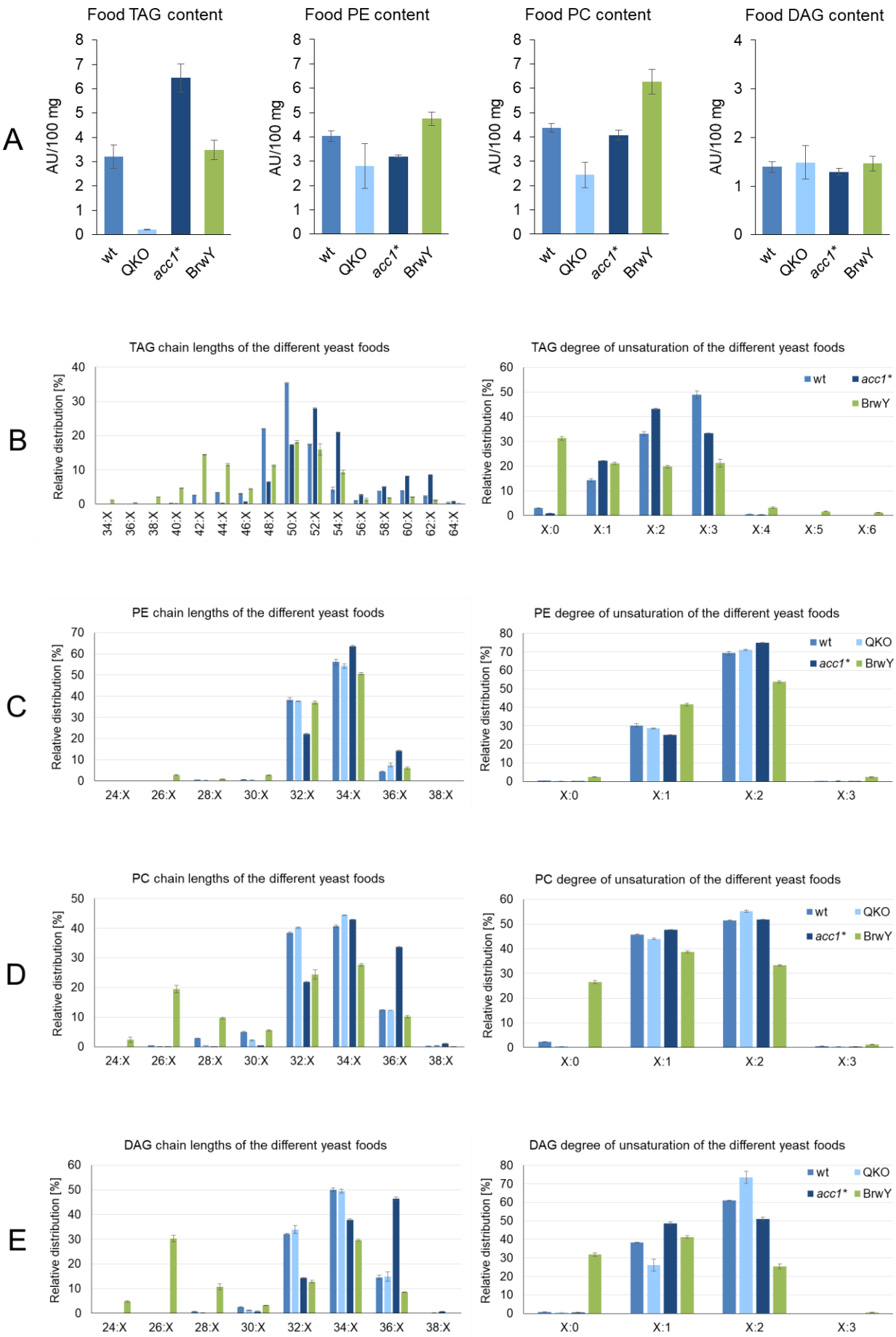
A
Food TAG content
Food PE content
Food PC content
Food DAG content
AU/100 mg
wt
QKO
acc1*
BrwY
B
TAG chain lengths of the different yeast foods
TAG degree of unsaturation of the different yeast foods
Relative distribution [%]
C
PE chain lengths of the different yeast foods
PE degree of unsaturation of the different yeast foods
D
PC chain lengths of the different yeast foods
PC degree of unsaturation of the different yeast foods
E
DAG chain lengths of the different yeast foods
DAG degree of unsaturation of the different yeast foods

Figure 5: **Total lipid contents, acyl chain length distribution and degree of unsaturation for the TAGs, PEs, PCs and DAGs found in the different yeast foods.** (**A**) Total TAG, PE, PC and DAG contents of the foods used in the experiments. The total amounts were calculated semi-quantitatively. The data shows the absolute amount in arbitrary units per 100 mg of wet yeast. (**B**) Grouping of TAGs into their respective acyl chain lengths (left) and degree of unsaturation (right) for the different yeast food sources in relative amounts of total TAG content. The relative TAG data for the QKO mutant was omitted as this yeast strain lacks this lipid class. (**C**) Grouping of PEs into their respective acyl chain lengths (left) and degree of unsaturation (right) for the different yeast food sources. (**D**) Grouping of PCs into their respective acyl chain lengths (left) and degree of unsaturation (right) for the different yeast food sources. (**E**) Grouping of DAGs into their respective acyl chain lengths (left) and degree of unsaturation (right) for the different yeast food sources. Data is shown as mean ± standard deviation of the mean. Sample size: n=3 for the *S. cerevisiae* strains, n=4 for the brewer's yeast.

Impact of different yeast foods on the *Drosophila* lipidome

In order to investigate the consequences of the characterised yeast strains on the lipidome of *Drosophila*, lipid profiling was performed in freshly eclosed (1d) and one-week old (7d) control males and mutant males lacking the major TAG lipase, Brummer (bmm^1) [38], reared on the described yeast foods from egg laying on (Figure 2). Notably, no physiological abnormalities nor substantial developmental delays were observed during fly development from embryogenesis over larval stages to the adult fly compared to flies reared on standard food (Dr. Harald Hofbauer, personal communication). This approach focuses on profiling the key storage lipid TAG, the major membrane lipids PE and PC, as well as the lipid transport molecule DAG.

Triacylglycerol (TAG) levels

Figure 6 shows the total TAG contents, distribution of TAG acyl chain lengths and degree of unsaturation of the control and bmm^1 flies 1 day and 7 days after eclosion. As seen in Figure 6A, bmm^1 flies accumulated TAG already prior to eclosion (panel 3) compared to control flies (panel 1). Both the control and the bmm^1 flies got leaner until day 7, however, the effect was more pronounced for the control flies compared to the bmm^1 flies (panel 2 and panel 4). The distribution of TAG acyl chain lengths of 1 day old control flies, shown in Figure 6B, showed a similar distribution for the different foods. It may be noted that flies raised on the *acc1** mutant yeast had slightly longer acyl chains compared to flies raised on other foods, which is in line with the observed longer acyl chains esterified in the lipid molecules of this yeast mutant strain (Figure 5B). A comparison regarding TAG acyl chain composition of control flies and bmm^1 flies 1 day after eclosion showed similar results for both genotypes. Interestingly, comparing these flies on day 7 (Figure 6C) revealed a shift in the acyl chain lengths towards TAG species with shorter acyl chains. This shift was much stronger for the control flies than for the bmm^1 flies, indicating a substantial contribution of storage TAG mobilisation to lipid homeostasis. The TAG

degree of unsaturation was quite similar between flies raised on different foods. Control and *bmm*^{1} flies raised on *acc1** yeast showed a slightly higher degree of unsaturation 1 day after eclosion displayed by an increase in X:3 species, whereas flies fed with brewer's yeast had elevated amounts of X:1 species compared to flies fed with the wild type and QKO strains (Figure 6D). 7 days after eclosion the flies showed almost the same degree of unsaturation for all different yeast foods (Figure 6E).

Taken together, *Drosophila* males showed very similar TAG levels and composition patterns independently of the food source. Interestingly, even serving the QKO mutant – completely lacking TAG – as sole food source resulted in a similar TAG content of the eclosed flies compared to the other yeast foods. Only the shift towards TAG species with longer acyl chains using the *acc1** strain was still reflected in the TAG profile of *Drosophila*. These data suggest that food-derived lipid processing and concomitant lipid remodelling have a much stronger influence on the TAG composition than diverse yeast food compositions.

A

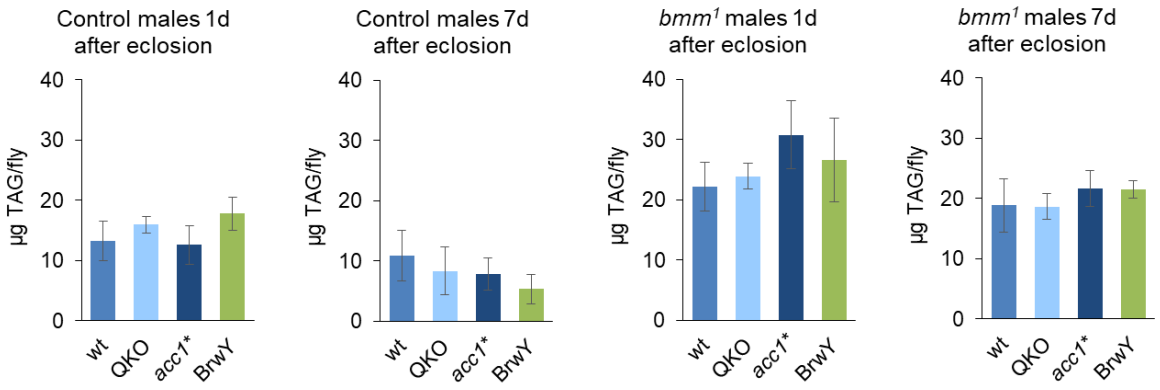
Control males 1d after eclosion
Control males 7d after eclosion
bmm¹ males 1d after eclosion
bmm¹ males 7d after eclosion
µg TAG/fly
0
10
20
30
40
wt
QKO
acc1*
BrwY

B

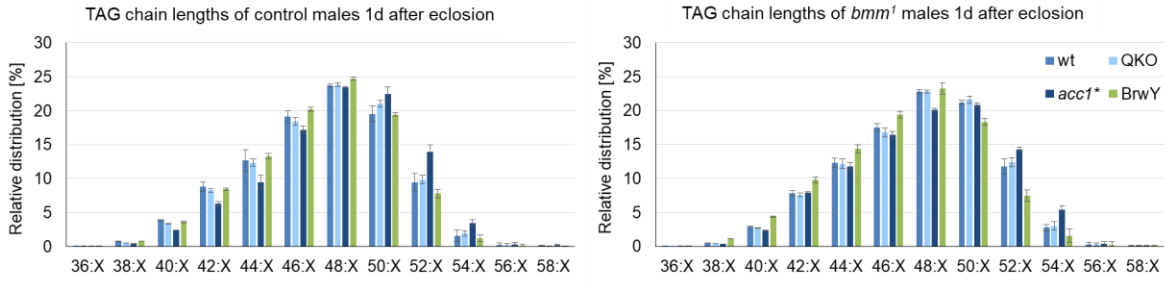
TAG chain lengths of control males 1d after eclosion
TAG chain lengths of bmm¹ males 1d after eclosion
Relative distribution [%]
0
5
10
15
20
25
30
36:X
38:X
40:X
42:X
44:X
46:X
48:X
50:X
52:X
54:X
56:X
58:X
wt
QKO
acc1*
BrwY

C

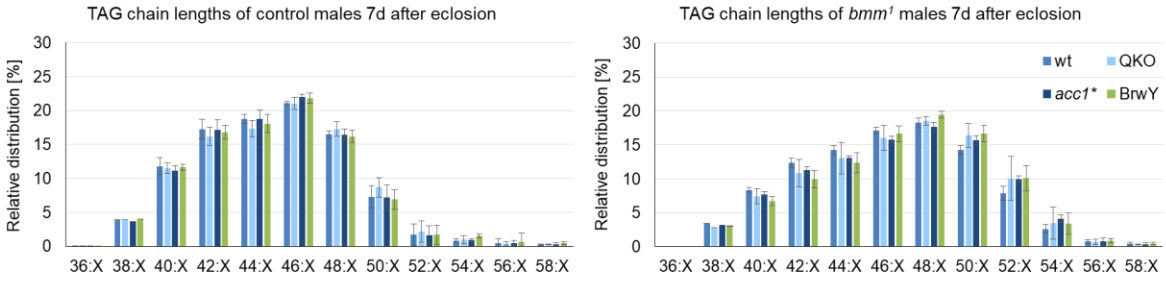
TAG chain lengths of control males 7d after eclosion
TAG chain lengths of bmm¹ males 7d after eclosion
Relative distribution [%]
0
5
10
15
20
25
30
36:X
38:X
40:X
42:X
44:X
46:X
48:X
50:X
52:X
54:X
56:X
58:X
wt
QKO
acc1*
BrwY

D

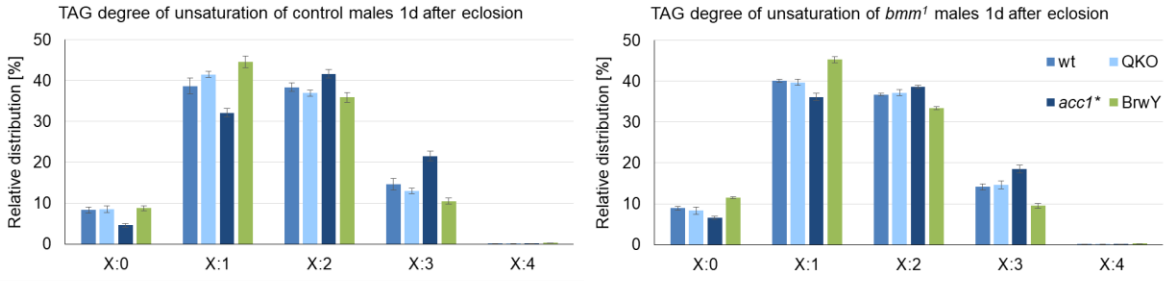
TAG degree of unsaturation of control males 1d after eclosion
TAG degree of unsaturation of bmm¹ males 1d after eclosion
Relative distribution [%]
0
10
20
30
40
50
X:0
X:1
X:2
X:3
X:4
wt
QKO
acc1*
BrwY

E

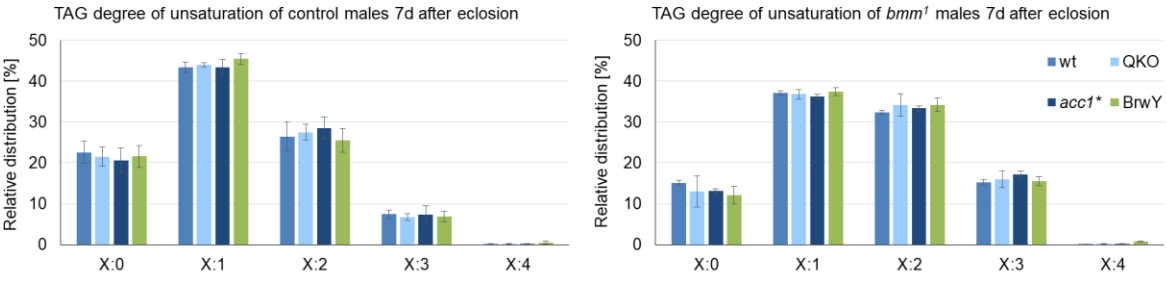
TAG degree of unsaturation of control males 7d after eclosion
TAG degree of unsaturation of bmm¹ males 7d after eclosion
Relative distribution [%]
0
10
20
30
40
50
X:0
X:1
X:2
X:3
X:4
wt
QKO
acc1*
BrwY

Figure 6: **Total TAG contents, TAG acyl chain length distribution and degree of unsaturation of control and *bmm*^{1} flies 1 day and 7 days after eclosion.** (**A**) Total TAG contents of the control and *bmm*^{1} flies 1 day and 7 days after eclosion. The absolute amounts were calculated using an internal standard of known concentration and are shown in µg TAG per fly. (**B**) Grouping of TAGs of 1 day old control (left) and *bmm*^{1} (right) flies into their respective acyl chain lengths plotted as relative amounts. (**C**) Grouping of TAGs of 7 days old control (left) and *bmm*^{1} (right) flies into their respective acyl chain lengths. (**D**) Grouping of TAGs of 1 day old control (left) and *bmm*^{1} (right) flies into their respective degree of unsaturation. (**E**) Grouping of TAGs of 7 days old control (left) and *bmm*^{1} (right) flies into their respective degree of unsaturation. Data is shown as mean ± standard deviation of the mean. Sample size: n=4 for the 1 day old QKO mutant-fed flies, n=5 for all others.

Phosphatidylethanolamine (PE) levels

Figure 7 shows the total PE contents, distribution of acyl chain lengths and degree of unsaturation of the control and *bmm*^{1} flies 1 day and 7 days after eclosion. As seen in Figure 7A, the amount of PE in the control flies decreased from one to seven days, while in the *bmm*^{1} flies the amount was quite constant, with the exception of the brewer's yeast-fed flies displaying a slight decrease in PE over time but also starting with elevated PE levels 1 day after eclosion. Noteworthy is the high variance in the 7 days old control flies that makes it difficult to assert the biological relevance of the decrease in the control flies. The distribution of PE chain lengths of 1 day old control flies, shown in Figure 7B, showed a similar distribution for the different foods. Flies raised on the *acc1** yeast had on average slightly longer PE acyl chains compared to flies raised on other yeasts. A comparison of control flies and *bmm*^{1} flies 1 day after eclosion showed almost identical results. Comparing these flies with 7 days old flies (Figure 7C) revealed a slight shift in PE acyl chain lengths towards 36:X species at the expense of 32:X and 34:X species, which can be observed for both the control and the *bmm*^{1} flies. The PE degree of unsaturation for 1 day old control flies (Figure 7D) showed same amounts of X:1 and X:2 PE species, independent of the food source. For the brewer's yeast-fed flies, low amounts of X:3 were detected, which were not present in flies fed with the *S. cerevisiae* strains. For the 1 day old *bmm*^{1} flies, similar distributions between all the yeast foods were found with slightly higher amounts of X:1 than X:2 species. Again, X:3 PE species were only detected in flies fed with brewer's yeast. As seen in Figure 7E, 7 days after eclosion, the control and *bmm*^{1} flies raised on all different foods shifted to around double the amount of X:2 compared to X:1 PE species.

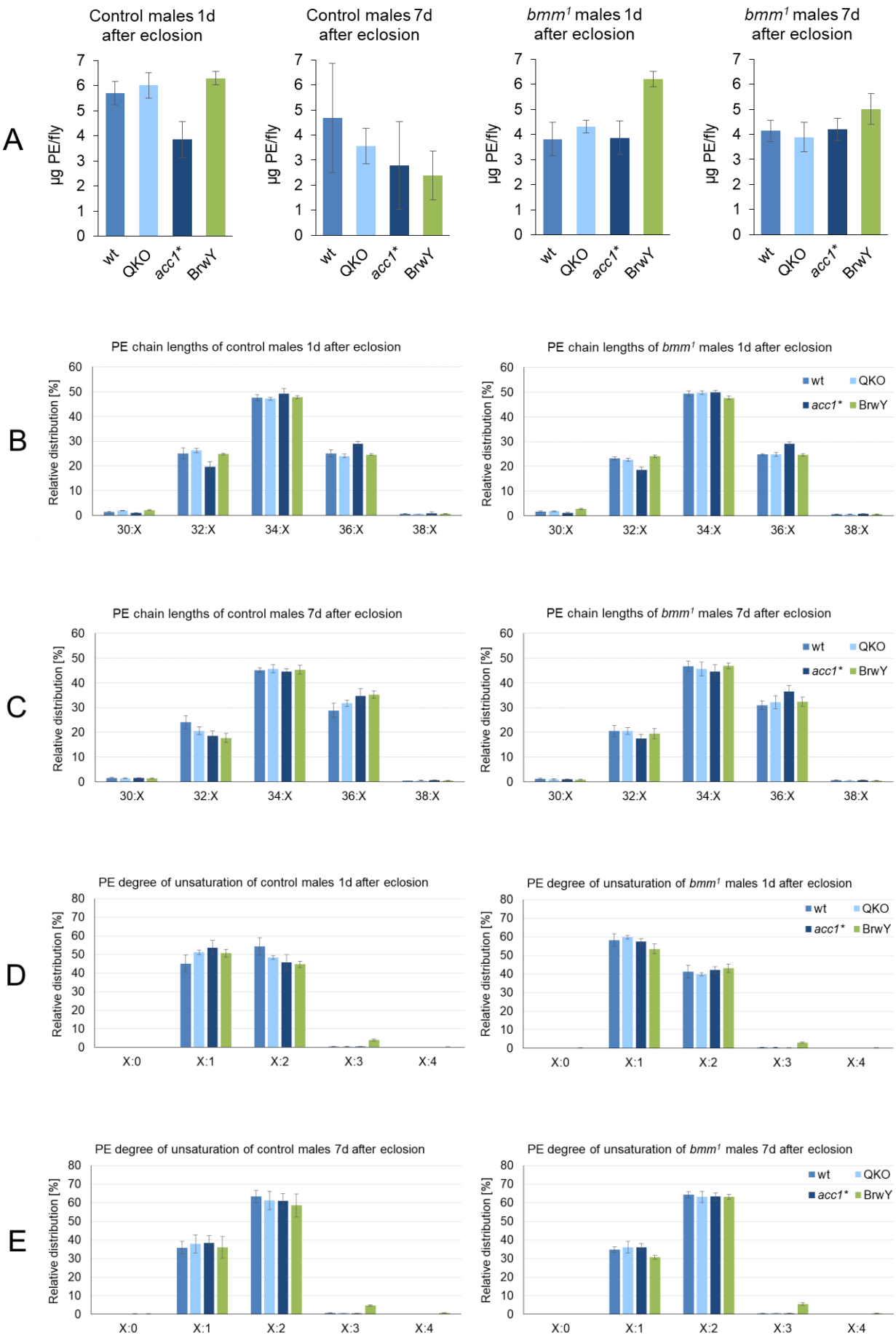
A
Control males 1d after eclosion
Control males 7d after eclosion
bmm1 males 1d after eclosion
bmm1 males 7d after eclosion
µg PE/fly
wt
QKO
acc1*
BrwY
B
PE chain lengths of control males 1d after eclosion
PE chain lengths of bmm1 males 1d after eclosion
C
PE chain lengths of control males 7d after eclosion
PE chain lengths of bmm1 males 7d after eclosion
D
PE degree of unsaturation of control males 1d after eclosion
PE degree of unsaturation of bmm1 males 1d after eclosion
E
PE degree of unsaturation of control males 7d after eclosion
PE degree of unsaturation of bmm1 males 7d after eclosion
Relative distribution [%]
30:X
32:X
34:X
36:X
38:X
X:0
X:1
X:2
X:3
X:4

Figure 7: **Total PE contents, PE acyl chain length distribution and degree of unsaturation of control and *bmm*^{1} flies 1 day and 7 days after eclosion.** (**A**) Total PE contents of the control and *bmm*^{1} flies 1 day and 7 days after eclosion. The absolute amounts were calculated using an internal standard of known concentration and are shown in µg PE per fly. (**B**) Grouping of PEs of 1 day old control (left) and *bmm*^{1} (right) flies into their respective acyl chain lengths plotted as relative amounts. (**C**) Grouping of PEs of 7 days old control (left) and *bmm*^{1} (right) flies into their respective acyl chain lengths. (**D**) Grouping of PEs of 1 day old control (left) and *bmm*^{1} (right) flies into their respective degree of unsaturation. (**E**) Grouping of PEs of 7 days old control (left) and *bmm*^{1} (right) flies into their respective degree of unsaturation. Data is shown as mean ± standard deviation of the mean. Sample size: n=4 for the 1 day old QKO mutant-fed flies, n=5 for all others.

Phosphatidylcholine (PC) levels

Figure 8 shows the total PC contents, distribution of acyl chain lengths and degree of unsaturation of the control and *bmm*^{1} flies 1 day and 7 days after eclosion. As seen in Figure 8A, the amount of PC in the control flies decreased from one to seven days, while in the *bmm*^{1} flies the amount was roughly the same, with the exception of the brewer's yeast-fed flies displaying a decrease in total PC over time, which was also observed for the PE levels. The distribution of PC acyl chain lengths of 1 day old control flies, shown in Figure 8B, was quite similar for the different foods. Notably, flies raised on the *acc1** yeast had on average slightly longer acyl chains in PC molecules 1 day after eclosion compared to flies raised on other yeasts. *bmm*^{1} flies 1 day after eclosion showed similar results as the control flies and a comparison of 1 day old flies with 7 days old flies (Figure 8C) revealed almost no difference in acyl chain length distribution. The PC degree of unsaturation for 1 day old control flies (Figure 8D) showed higher amounts of X:2 compared to X:1 for all different foods. For the brewer's yeast-fed flies low amounts of X:3 species were detected, which are not present in flies fed with the *S. cerevisiae* strains. For the 1 day old *bmm*^{1} flies, similar distributions between all the yeast foods were detected with almost equal amounts of X:1 and X:2, which remained constant until 7 days after eclosion. As observed in control males, PC X:3 species were only detected in flies fed with brewer's yeast. 7 days after eclosion, the PC X:1 level in the control flies raised to reach a similar amount as the X:2 PC species, independent of the yeast strain (Figure 8E).

In conclusion, *Drosophila* males showed quite similar PE and PC levels and composition patterns independently of the food source. Only the shift towards longer acyl chains using the *acc1** mutant strain was still reflected in the PL profile of *Drosophila.* These data suggest that membrane lipids undergo much less remodelling from 1 day to 7 days after eclosion when compared with the TAG profiles, indicating that membrane lipid homeostasis is more tightly regulated than storage TAG levels.

A

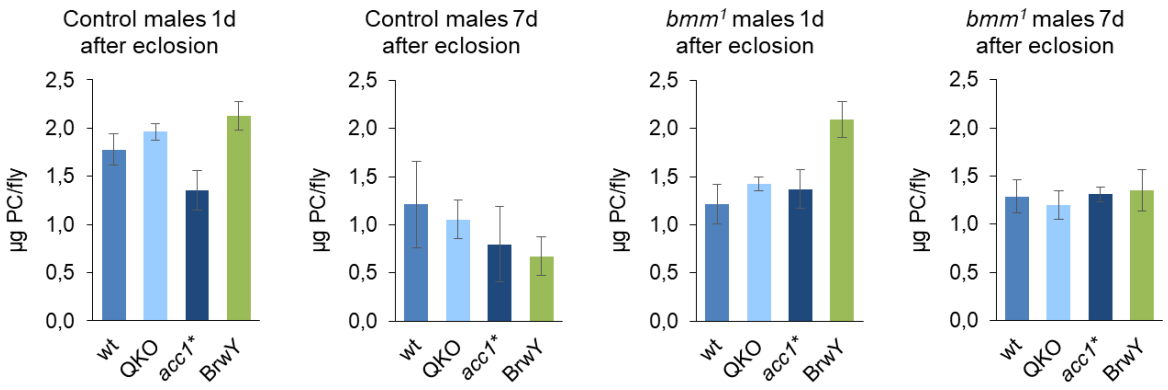
Control males 1d after eclosion
Control males 7d after eclosion
bmm1 males 1d after eclosion
bmm1 males 7d after eclosion
µg PC/fly
2,5
2,0
1,5
1,0
0,5
0,0
wt
QKO
acc1*
BrwY

B

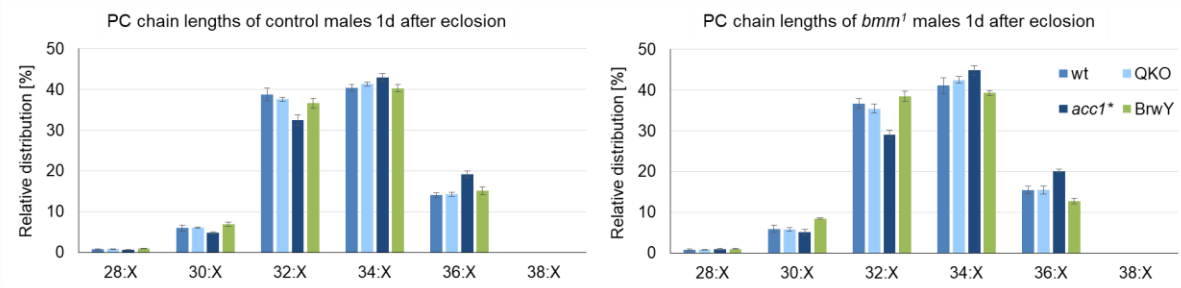
PC chain lengths of control males 1d after eclosion
PC chain lengths of bmm1 males 1d after eclosion
Relative distribution [%]
50
40
30
20
10
0
28:X
30:X
32:X
34:X
36:X
38:X
wt
QKO
acc1*
BrwY

C

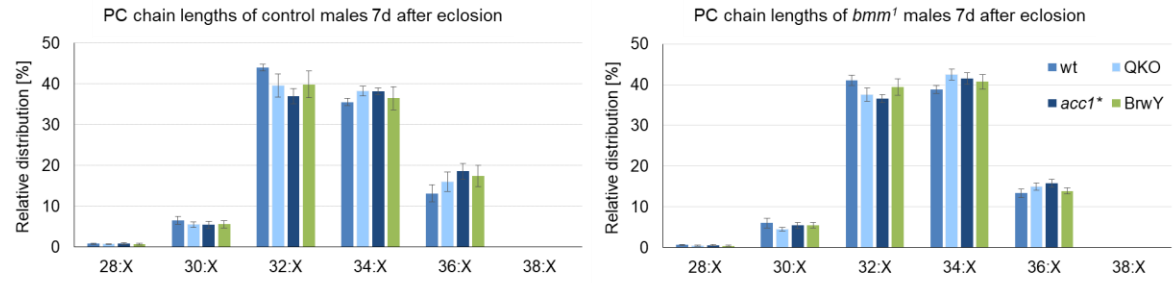
PC chain lengths of control males 7d after eclosion
PC chain lengths of bmm1 males 7d after eclosion
Relative distribution [%]
50
40
30
20
10
0
28:X
30:X
32:X
34:X
36:X
38:X
wt
QKO
acc1*
BrwY

D

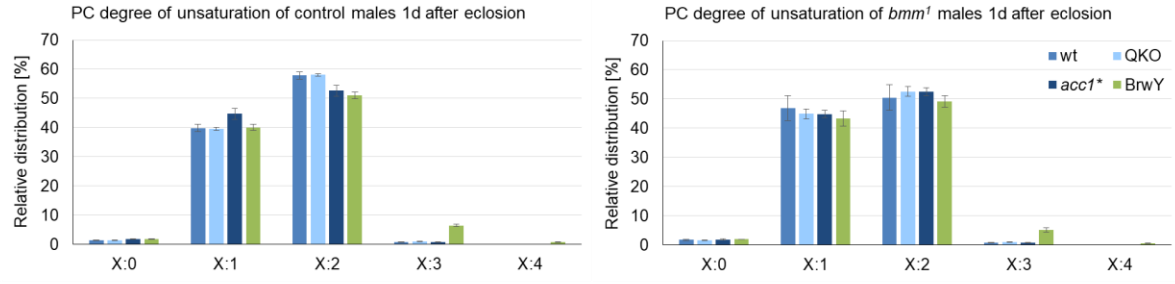
PC degree of unsaturation of control males 1d after eclosion
PC degree of unsaturation of bmm1 males 1d after eclosion
Relative distribution [%]
70
60
50
40
30
20
10
0
X:0
X:1
X:2
X:3
X:4
wt
QKO
acc1*
BrwY

E

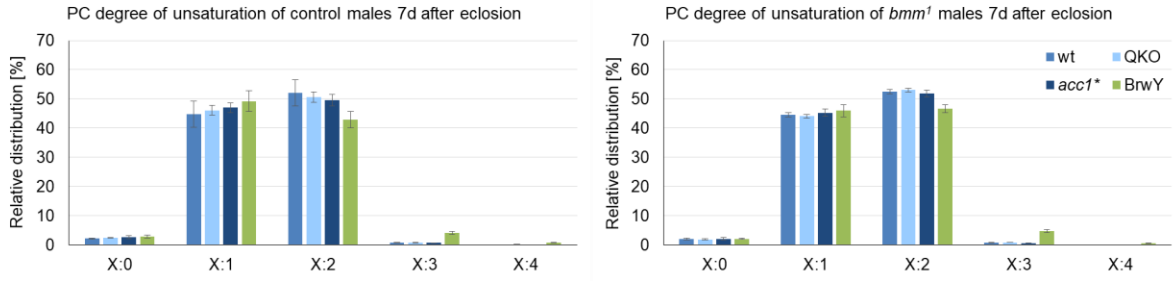
PC degree of unsaturation of control males 7d after eclosion
PC degree of unsaturation of bmm1 males 7d after eclosion
Relative distribution [%]
70
60
50
40
30
20
10
0
X:0
X:1
X:2
X:3
X:4
wt
QKO
acc1*
BrwY

Figure 8: **Total PC contents, PC acyl chain length distribution and degree of unsaturation of control and *bmm*^{1} flies 1 day and 7 days after eclosion.** (**A**) Total PC contents of the control and *bmm*^{1} flies 1 day and 7 days after eclosion. The absolute amounts were calculated using an internal standard of known concentration and are shown in µg PC per fly. (**B**) Grouping of PCs of 1 day old control (left) and *bmm*^{1} (right) flies into their respective acyl chain lengths plotted as relative amounts. (**C**) Grouping of PCs of 7 days old control (left) and *bmm*^{1} (right) flies into their respective acyl chain lengths. (**D**) Grouping of PCs of 1 day old control (left) and *bmm*^{1} (right) flies into their respective degree of unsaturation. (**E**) Grouping of PCs of 7 days old control (left) and *bmm*^{1} (right) flies into their respective degree of unsaturation. Data is shown as mean ± standard deviation of the mean. Sample size: n=4 for the 1 day old QKO mutant-fed flies, n=5 for all others.

Diacylglycerol (DAG) levels

Figure 9 shows the total DAG contents, distribution of acyl chain lengths and degree of unsaturation of the control and *bmm*^{1} flies 1 day and 7 days after eclosion. As seen in Figure 9A, the amount of DAG in both the control flies and the *bmm*^{1} flies decreased from one to seven days. The distribution of DAG acyl chain lengths of 1 day old control flies, illustrated in Figure 9B, showed a similar distribution for the different foods. Flies raised on the *acc1** mutant yeast had slightly longer acyl chains compared to flies raised on other foods. A comparison of control flies and *bmm*^{1} flies 1 day after eclosion showed similar results. Comparing these flies with 7 days old flies (Figure 9C) shows that there was a shift in acyl chain lengths towards shorter DAG molecules, which was much stronger for the control flies than the *bmm*^{1} flies, also in line with the observed shifts in the TAG profiles. The degree of unsaturation for 1 day old control flies (Figure 9D) was similar for all different foods, with the wild type- and *acc1**-fed flies having slightly more saturated DAGs. The *bmm*^{1} flies had a similar degree of unsaturation for all different foods and a slightly higher degree of unsaturation compared to the control flies. As seen in Figure 9E, 7 days after eclosion, both the control and *bmm*^{1} flies shifted towards more saturated DAG molecules, which was much more pronounced for the control flies.

Taken together, *Drosophila* males showed very similar DAG levels and composition patterns independently of the food source. Only the shift towards longer acyl chains using the *acc1** mutant strain was still reflected in the DAG profile of *Drosophila*. Notably, the DAG profiles and the changes in the DAG profiles from 1 day to 7 days strongly resemble the changes observed in the TAG profile.

A

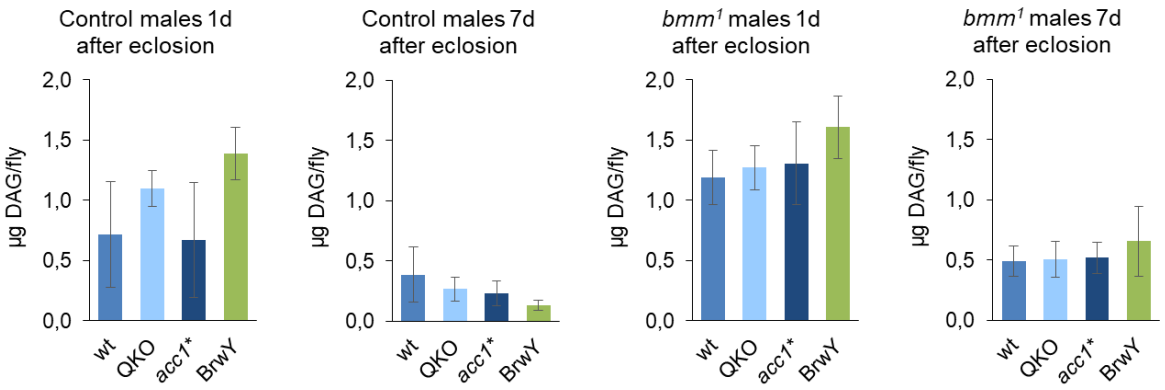
Control males 1d after eclosion
Control males 7d after eclosion
bmm¹ males 1d after eclosion
bmm¹ males 7d after eclosion
µg DAG/fly
2,0
1,5
1,0
0,5
0,0
wt
QKO
acc1*
BrwY

B

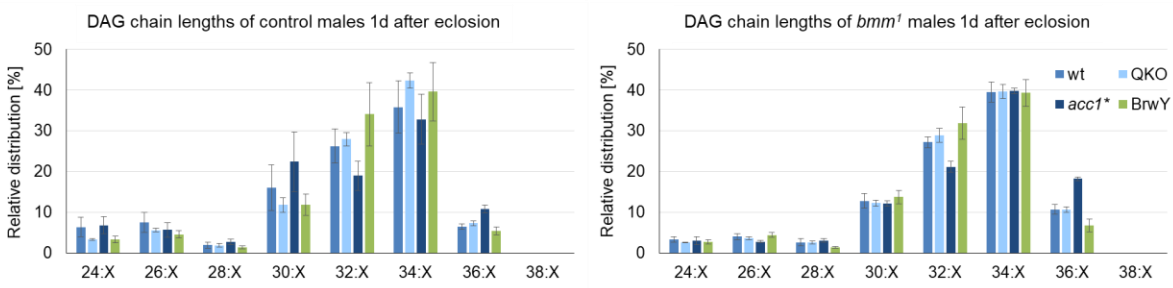
DAG chain lengths of control males 1d after eclosion
DAG chain lengths of bmm¹ males 1d after eclosion
Relative distribution [%]
50
40
30
20
10
0
24:X
26:X
28:X
30:X
32:X
34:X
36:X
38:X
wt
QKO
acc1*
BrwY

C

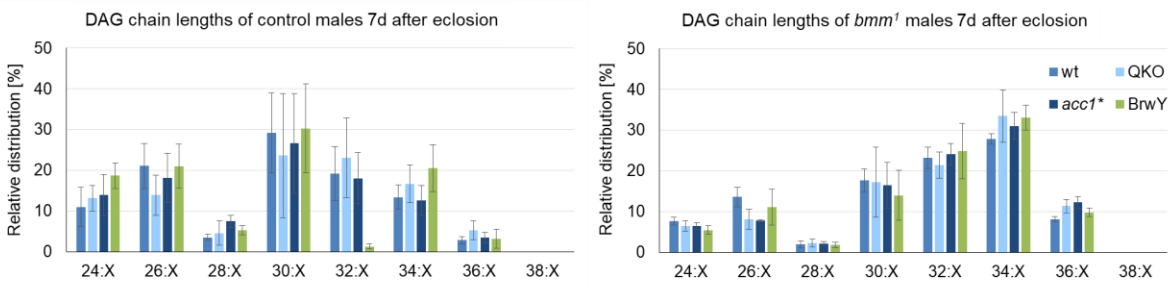
DAG chain lengths of control males 7d after eclosion
DAG chain lengths of bmm¹ males 7d after eclosion
Relative distribution [%]
50
40
30
20
10
0
24:X
26:X
28:X
30:X
32:X
34:X
36:X
38:X
wt
QKO
acc1*
BrwY

D

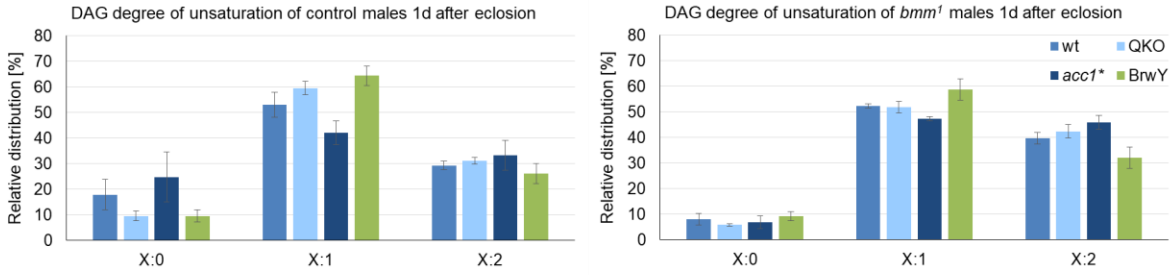
DAG degree of unsaturation of control males 1d after eclosion
DAG degree of unsaturation of bmm¹ males 1d after eclosion
Relative distribution [%]
80
70
60
50
40
30
20
10
0
X:0
X:1
X:2
wt
QKO
acc1*
BrwY

E

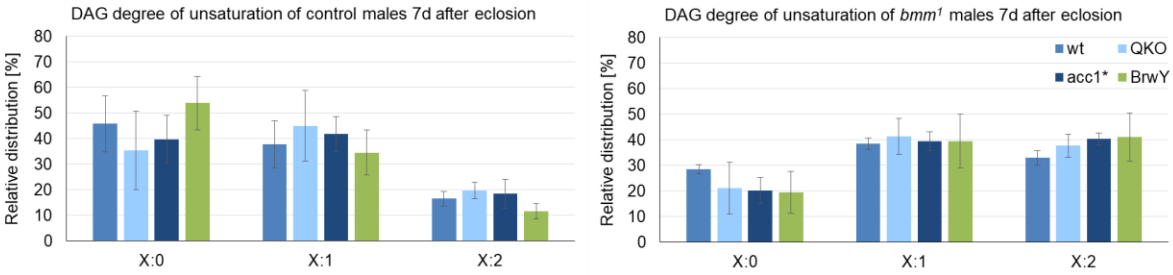
DAG degree of unsaturation of control males 7d after eclosion
DAG degree of unsaturation of bmm¹ males 7d after eclosion
Relative distribution [%]
80
70
60
50
40
30
20
10
0
X:0
X:1
X:2
wt
QKO
acc1*
BrwY

Figure 9: **Total DAG contents, DAG acyl chain length distribution and degree of unsaturation of control and *bmm*^{1} flies 1 day and 7 days after eclosion.** (**A**) Total DAG contents of the control and *bmm*^{1} flies 1 day and 7 days after eclosion. The absolute amounts were calculated using an internal standard of known concentration and are shown in µg DAG per fly. (**B**) Grouping of DAGs of 1 day old control (left) and *bmm*^{1} (right) flies into their respective acyl chain lengths plotted as relative amounts. (**C**) Grouping of DAGs of 7 days old control (left) and *bmm*^{1} (right) flies into their respective acyl chain lengths. (**D**) Grouping of DAGs of 1 day old control (left) and *bmm*^{1} (right) flies into their respective degree of unsaturation. (**E**) Grouping of DAGs of 7 days old control (left) and *bmm*^{1} (right) flies into their respective degree of unsaturation. Data is shown as mean ± standard deviation of the mean. Sample size: n=4 for the 1 day old QKO mutant-fed flies, n=5 for all others.

Faeces analysis

To estimate the amount of TAGs (and possibly other relevant lipids) in the faeces samples prior to injection into the UPLC-qTOF-MS, thin-layer chromatography was performed. Figure 10 shows a representative thin-layer chromatogram of two blank extractions (lanes 2 and 3) and of dedicated faeces samples (lanes 4-7) all bearing strong bands close to the solvent front with a retention factor (R_f) value of 0.88, which occurred slightly higher than the cholesterol ester band of the used standard mix (lane 1). All faeces samples showed very light bands at approximately the same retention time as the TAG standard (R_f 0.52). An additional band specific for faeces from males (R_f 0.60, lanes 4 and 6) appeared slightly higher than the TAG standard, which was absent in the faeces from females (lanes 5 and 7). Other bands appeared at R_f 0.38 in all faeces samples, which yet remain to be characterised, and at R_f 0.16, potentially representing free fatty acids. The band at the same height as the cholesterol of the standard mix (R_f 0.08) might also include DAG besides the free sterols. Due to the fact that these two substances don't diverge properly, it is not possible to characterise the substance without further analyses.

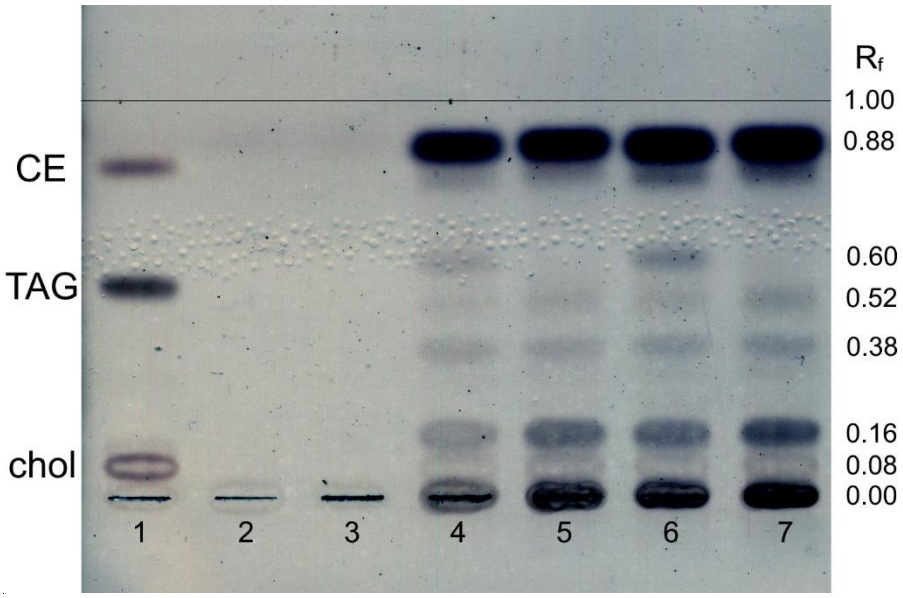

Figure 10: **Thin layer chromatogram of faeces samples.** The samples from left to right: (**1**) Standard, (**2**) Blank extraction 1, (**3**) Blank extraction 2, (**4**) Faeces male wild type flies, (**5**) Faeces female wild type flies, (**6**) Faeces male *bmm*^{1} mutant flies, (**7**) Faeces female *bmm*^{1} mutant flies. Standard: CE … cholesterol ester, TAG … triacylglycerol, chol … cholesterol

In order to obtain more information on the nature of the visualised lipids from the thin-layer chromatogram, we performed UPLC-qTOF mass spectrometry analyses. The signal intensities of the lipids in the faeces samples were quite low. Figure 11 shows the comparison of the chromatograms of the blank extraction and a faeces sample of male *bmm*^{1} mutant flies, showing considerable amounts of triacylglycerol in the faeces sample. There are also detectable amounts of PLs and DAGs in the sample, however the amounts are quite low and are therefore not visible in the base peak chromatogram. The peak at RT 10.48 min has an m/z ratio of 515.4160, however, there are no database entries of relevant lipids that would yield an adduct ion of this m/z value.

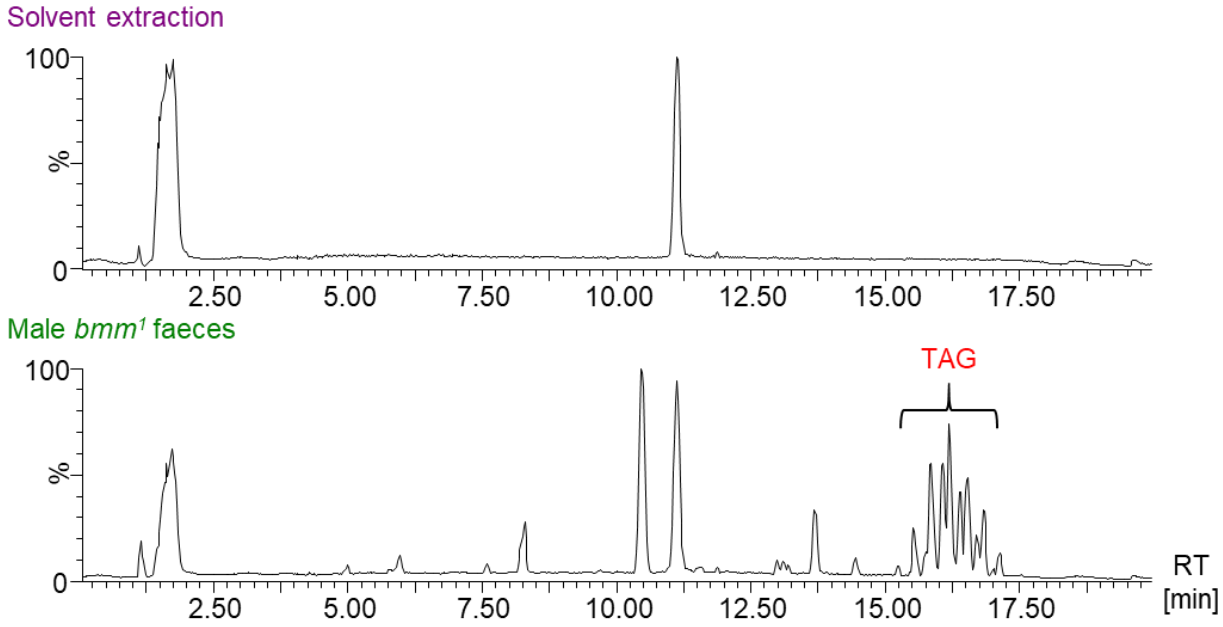

Figure 11: **Chromatograms of the blank extraction and faeces sample of the male *bmm*^{1} flies**. The solvent extraction contains known peaks at RT 1.74 min and RT 11.11 min, which both arise from the solvent. The faeces chromatogram shows considerable amounts of TAG and detectable, but in this depiction not visible, amounts of PL and DAG species.

Figure 12 shows TAG, PE, PC and DAG contents of the faeces samples of control and *bmm*^{1} males and a blank extraction (Figure 12A), as well as the distribution of acyl chain lengths and degree of unsaturation within these lipid classes (Figure 12B-E). Addition of internal standards was omitted to prevent masking of naturally occurring lipid species, hence, lipid amounts are plotted semi-quantitatively as arbitrary units. The *bmm*^{1} fly faeces contained higher amounts of TAG, but lower amounts of the PLs and DAGs compared to the control fly faeces (Figure 12A). The distributions of all lipids regarding acyl chain length distribution and degree of unsaturation were essentially the same for the control and *bmm*^{1} faeces samples. Interestingly, the distribution of TAG acyl chain lengths showed high amounts of TAG species with long acyl chains (Figure 12B), with 54:X being the predominant chain length for the TAG molecules. The degree of unsaturation for the TAGs resembled a Gaussian distribution with X:4 at its peak. The phospholipids PE and PC, seen in the Figures 12C and 12D, contained almost exclusively 32:X, 34:X and 36:X species with a degree of unsaturation of X:1 or X:2. The PC molecules showed a slightly longer average acyl chain length and higher amounts of X:2 compared to the PE molecules. Both the PCs and PEs also contained X:3 and X:4 species. Surprisingly, the DAGs were composed of mostly 34:X and 36:X species (Figure 12E), however there were moderate amounts of 26:X, 28:X and 32:X DAGs and the degree of unsaturation showed DAG molecules ranging from X:0 to X:4.

Taken together, the TAG and DAG species found in the *Drosophila* faeces had longer acyl chains compared to their counterparts in the *Drosophila* lipidome and a wide distribution of the degree of unsaturation, whereas the phospholipids showed almost the same patterns as the food and the *Drosophila* lipid profiles.

A

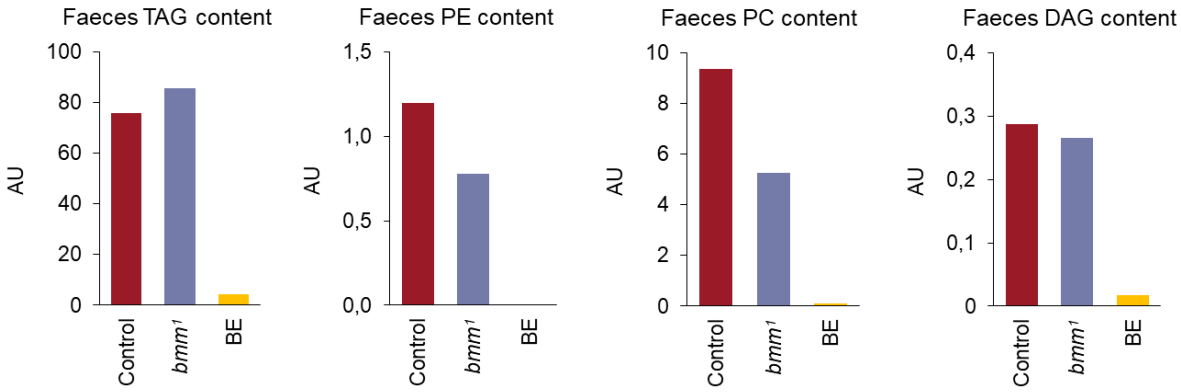
Faeces TAG content
AU
100
80
60
40
20
0
Control
bmm1
BE
Faeces PE content
AU
1,5
1,0
0,5
0,0
Control
bmm1
BE
Faeces PC content
AU
10
8
6
4
2
0
Control
bmm1
BE
Faeces DAG content
AU
0,4
0,3
0,2
0,1
0
Control
bmm1
BE

B

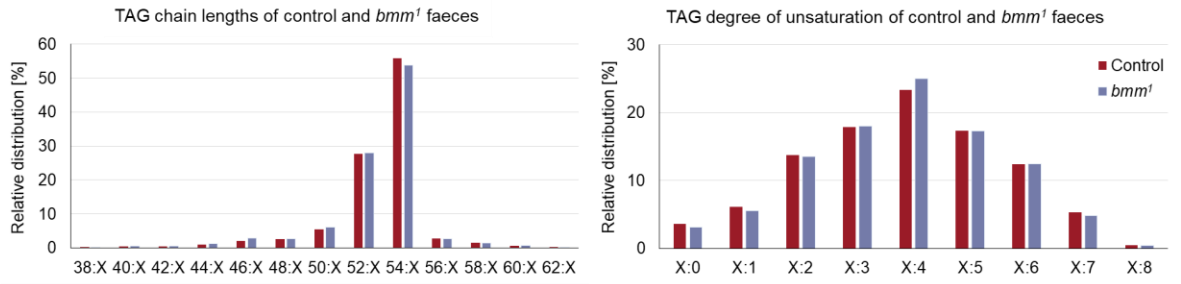
TAG chain lengths of control and bmm1 faeces
Relative distribution [%]
60
50
40
30
20
10
0
38:X 40:X 42:X 44:X 46:X 48:X 50:X 52:X 54:X 56:X 58:X 60:X 62:X
TAG degree of unsaturation of control and bmm1 faeces
Relative distribution [%]
30
20
10
0
Control
bmm1
X:0 X:1 X:2 X:3 X:4 X:5 X:6 X:7 X:8

C

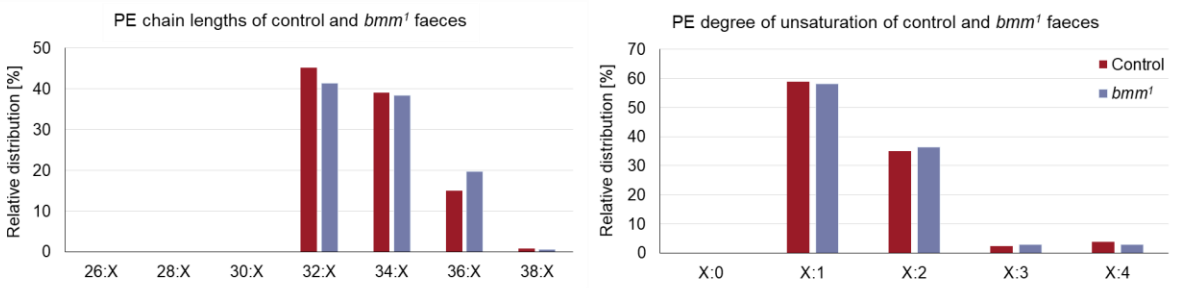
PE chain lengths of control and bmm1 faeces
Relative distribution [%]
50
40
30
20
10
0
26:X 28:X 30:X 32:X 34:X 36:X 38:X
PE degree of unsaturation of control and bmm1 faeces
Relative distribution [%]
70
60
50
40
30
20
10
0
Control
bmm1
X:0 X:1 X:2 X:3 X:4

D

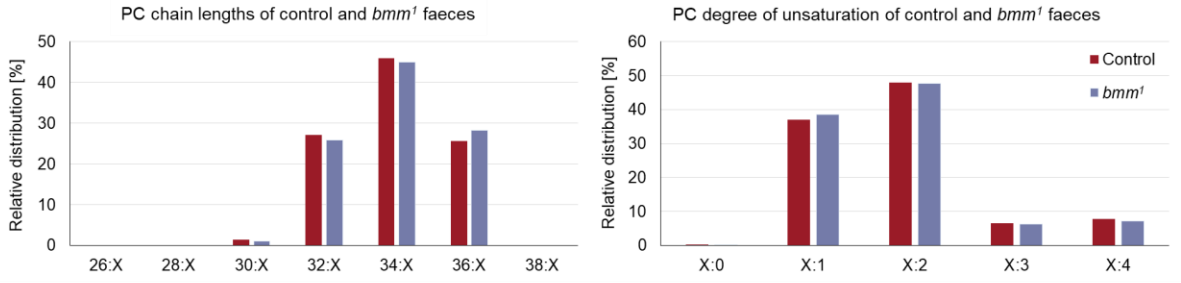
PC chain lengths of control and bmm1 faeces
Relative distribution [%]
50
40
30
20
10
0
26:X 28:X 30:X 32:X 34:X 36:X 38:X
PC degree of unsaturation of control and bmm1 faeces
Relative distribution [%]
60
50
40
30
20
10
0
Control
bmm1
X:0 X:1 X:2 X:3 X:4

E

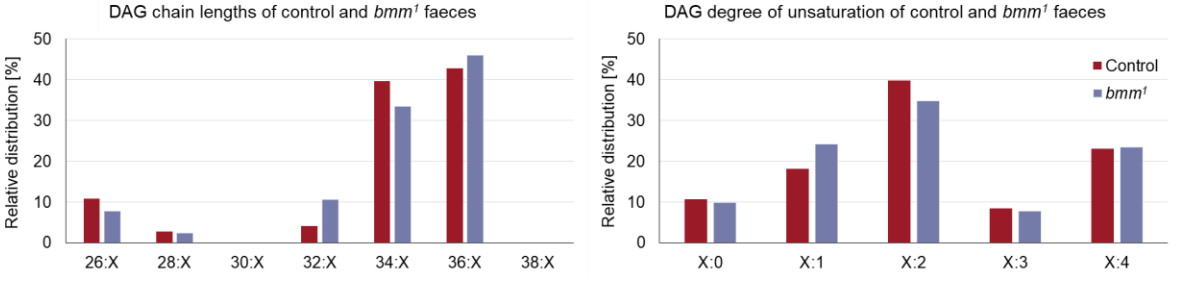
DAG chain lengths of control and bmm1 faeces
Relative distribution [%]
50
40
30
20
10
0
26:X 28:X 30:X 32:X 34:X 36:X 38:X
DAG degree of unsaturation of control and bmm1 faeces
Relative distribution [%]
50
40
30
20
10
0
Control
bmm1
X:0 X:1 X:2 X:3 X:4

Figure 12: **Total lipid contents, acyl chain length distribution and degree of unsaturation for the TAGs, PEs, PCs and DAGs in faeces samples of control and *bmm*^{1} males.** (**A**) Total TAG, PE, PC and DAG contents of the control and *bmm*^{1} faeces samples. The data shows the total amount in arbitrary units given by the LDA software. No internal standard was used for the faeces samples. (**B**) Grouping of TAGs into their respective acyl chain lengths (left) and degree of unsaturation (right) for the control and *bmm*^{1} faeces samples plotted as relative amounts. (**C**) Grouping of PEs into their respective acyl chain lengths (left) and degree of unsaturation (right) for the control and *bmm*^{1} faeces samples. (**D**) Grouping of PCs into their respective acyl chain lengths (left) and degree of unsaturation (right) for the control and *bmm*^{1} faeces samples. (**E**) Grouping of DAGs into their respective acyl chain lengths (left) and degree of unsaturation (right) for the control and *bmm*^{1} faeces samples. As the faeces analysis was a pilot test, the sample size was n=1, therefore no statistics are available.

Finally, Figure 13 shows a combined overview of the TAG acyl chain length distribution and degree of unsaturation starting with the brewer's yeast strain as food source (Figure 13A), followed by the TAG profiles of 1 day and 7 days old brewer's yeast-fed control and *bmm*^{1} *Drosophila* males (Figures 13B and 13C) and finally the TAG species found in the faeces of the brewer's yeast-fed control and *bmm*^{1} flies (Figure 13D). This direct comparison illustrates the remodelling of the TAG acyl chain lengths from food consumption to 1 day old flies, followed by a shift towards shorter TAG species in 7 days old flies as well as the excreted long chain TAG molecules that potentially remained unutilised during digestion. The Figure shall highlight the breakdown of long high-energy fatty acyl chains from yeast food by *Drosophila* and the adjustment to shorter TAG molecules. Furthermore, Brummer deficiency substantially delays further lipid remodelling from 1 day to 7 days old males and suggests a pivotal role of Brummer lipase on TAG mobilisation in young adult *Drosophila* males. The faeces TAG profile suggests that Drosophila is incapable of absorbing and metabolising long-chain poly-unsaturated TAGs, which will be the subject of future studies.

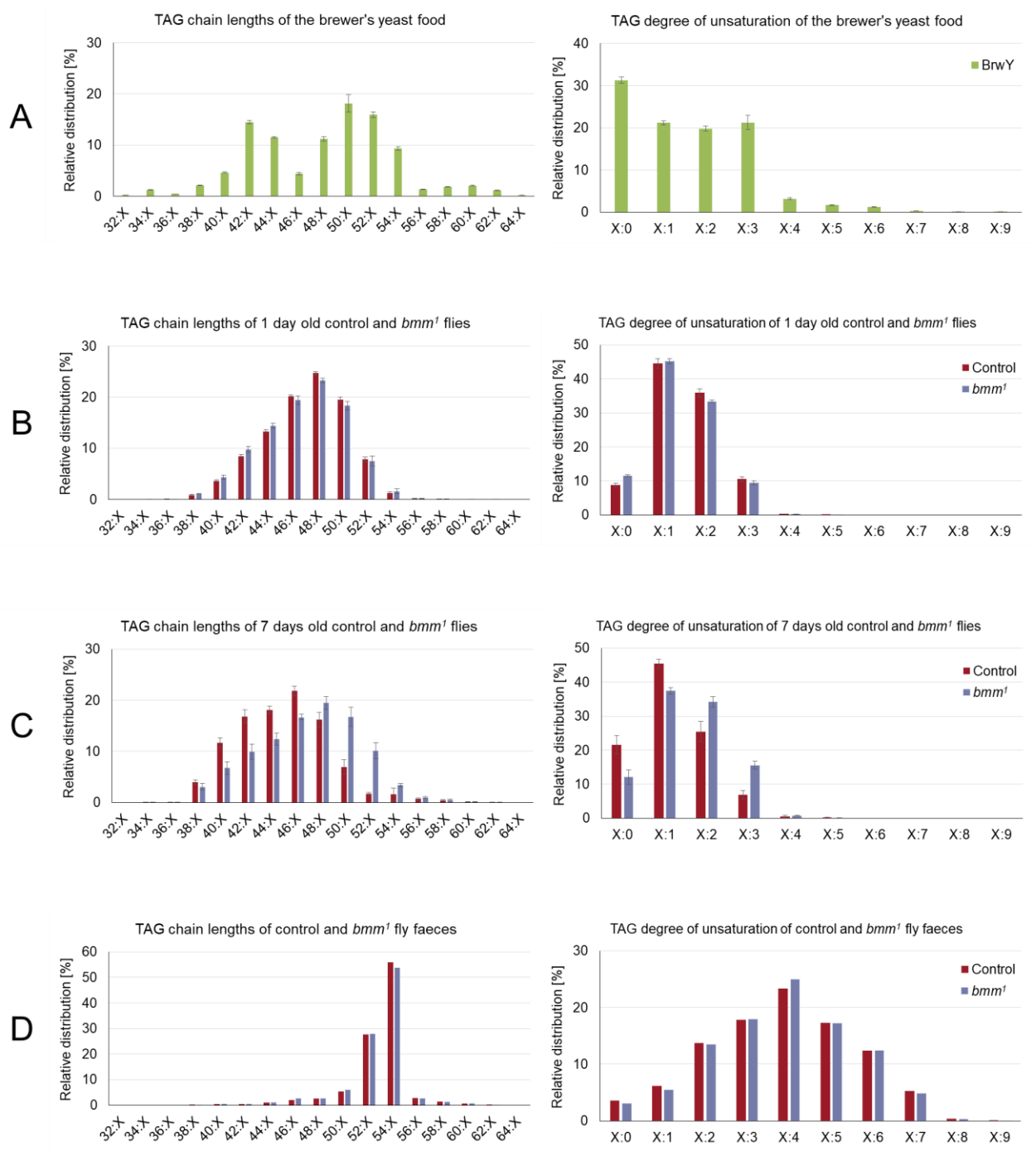

Figure 13: **Direct comparison of TAG species composition in food, fly and faeces.** The Figure shows the TAG chain length distribution and degree of unsaturation for the brewer's yeast (**A**), the brewer's yeast-fed 1 day old control and *bmm*^{1} males (**B**), the brewer's yeast-fed 7 days old control and *bmm*^{1} males (**C**) and the faeces of the brewer's yeast-fed control and *bmm*^{1} males (**D**). The data shows the relative amounts of TAGs with the same acyl chain length/degree of unsaturation. Data for the food and flies is shown as mean ± standard deviation of the mean. The sample sizes are: n=4 for the brewer's yeast, n=5 for the flies and n=1 for the faeces.

Discussion

The aim of this thesis was to study the effect of yeast foods with different lipid compositions, especially in regards to lipid content, acyl chain distribution and degree of unsaturation, on the lipidome of *Drosophila melanogaster* of two different genetic backgrounds, wild type *Drosophila* (w^{1118}) and *Drosophila* with impaired TAG mobilisation (bmm^{1}). Additionally, the lipid profile of the faeces was analysed, giving insight into the digestion process of dietary lipids in *Drosophila*.

Food lipidomic analyses proved the described phenotypes of the *S. cerevisiae* strains with regard to the total TAG contents. Compared to the laboratory wild type strain BCy907c, the QKO mutant lacks any TAGs due to chromosomal deletion of the genes *DGA1* and *LRO1*, which code for the diacylglycerol acyltransferases (DGAT) needed for TAG synthesis, as well as deletions of *ARE1* and *ARE2*, encoding for sterol acyltransferases that also show little DGAT activity [60], [61]. The *acc1** mutant has a higher TAG content and longer acyl chains, due to the hyperactivity of the enzyme acetyl-CoA carboxylase, which catalyses the conversion of acetyl-CoA into malonyl-CoA [62], therefore pushing the lipid synthesis towards longer fatty acyl chains and forcing the yeast to produce large amounts of lipid, which is then stored in the form of TAG in lipid droplets [64]. Noteworthy, our quality control experiments show that there are only negligible contaminations contributing to our measurements. The small amounts of lipid found in our blanks most likely arise either from background noise that was integrated by the LDA or from memory effects of residual lipids in the UPLC system. Since we calculated the lipid content per 100 mg of yeast wet weight, the brewer's yeast cannot be directly compared to the other yeast foods, as it is dry yeast that has been suspended in water, whereas the *S. cerevisiae* strains are life yeasts, where it can be assumed that they have similar wet weight densities. However, the yet uncharacterised brewer's yeast was included in this study as it is a component of the complex standard food used in the laboratory [66] and serves as the sole food source in ongoing studies for embryonic development. With regard to membrane lipids, the *S. cerevisiae* strains contain similar amounts of PE and PC, whereas the brewer's yeast shows higher PE and PC contents per 100 mg wet weight. Interestingly, the QKO mutant has lower amounts of phospholipids, despite being unable to store excess lipid metabolites in the form of TAG in lipid droplets. As there are other phospholipids present in the cell, it is possible that the genetic background of this mutant somehow shifts the equilibrium of phospholipids towards minor lipid classes such as PI and PS. Moreover, lipid droplets, the storage organelles for TAGs, are surrounded with a phospholipid monolayer and the lack of lipid droplets in the QKO strain might also contribute to decreased membrane lipid levels. However, since the overall goal was to serve food with low, medium and high TAG content to *Drosophila*, the choice of these yeast mutant strains was very appropriate. The distribution of TAG acyl chain lengths and degree of unsaturation for the used yeast strains shows longer fatty acyl chains esterified in all analysed lipid classes for the *acc1** mutant, which has already been described above, and a similar degree of unsaturation compared to our wild

type strain. For the brewer's yeast we observe a wide distribution of TAG acyl chain lengths ranging from 34:X to 64:X. The brewer's yeast is also the only yeast that contains fatty acids with more than three double bonds (X:4 to X:6). Due to its unknown origin, it is not clear, whether this type of yeast is capable of producing these fatty acids or if they derive from any kind of contamination of the dry yeast. For PE and PC, we have a similar distribution of fatty acyl chain lengths and degree of unsaturation for the wild type strain and the QKO mutant. Notably, the *acc1** mutant has on average slightly longer fatty acyl chains with a similar degree of unsaturation, which is in line with the observed alterations in the TAG species. In comparison, the brewer's yeast also contains low amounts of short PE and substantial amounts of short PC species (24:X to 30:X), that are almost absent in the *S. cerevisiae* strains. Furthermore, the brewer's yeast is the only strain containing X:3 PE species and a high amount of X:0 PC species. The DAG composition basically resembles the PC composition with regard to acyl chain length distribution and degree of unsaturation. Interestingly, the observed differences in the PL species pattern in the *acc1** mutant and the brewer's yeast were more pronounced in PC than in PE species, indicating that deregulation of PE homeostasis might be more detrimental than alterations in the PC species composition. Due to their small head group, PE molecules are capable of inducing negative membrane curvature, which could ultimately result in inverted hexagonal membrane phases that impair biological functions such as organellar compartmentalisation and trafficking events within living cells [52], [67]. The alterations in DAG, another lipid molecule with a small head group, might have less impact due to lower total amounts present in the cell as determined in this study. Taken together, we prepared and characterised a highly appropriate selection of yeast-based foods with low, medium and high TAG content, additionally bearing different fatty acyl chain length distributions and varying degrees of unsaturation in the analysed lipid classes for our rearing experiments using *Drosophila* males.

In order to investigate the impact of yeast-based food sources with different lipid content and lipid composition on the lipidome of adult *Drosophila* males, we allowed control and bmm^{1} females to lay ~100 eggs on agar/glucose plates with the abovementioned yeast strains as sole food source. Thus, after embryogenesis, the hatched larvae, which increase approximately 200-fold in body mass during larval development [68], solely rely on the served yeast food until pupariation. Total TAG content of 1 day old males was almost equal independent of the food source. Control males contain less TAG than bmm^{1} males, consistent with literature [38]. Astonishingly, the QKO strain – completely lacking TAG – results in the same TAG pattern as the other strains, indicating that the nature of the food-derived lipids is not crucial for normal fly development. The TAG species composition 1 day after eclosion is very similar on all food sources, meaning that during fly development, the acyl chain composition of the ingested yeast food is heavily adjusted to represent the lipidome of the eclosed fly. The differences in TAG acyl chain distribution and degree of unsaturation seen for the *acc1** mutant strain and the brewer's yeast are almost abolished in the TAG profile of freshly eclosed male flies. For example, the 58:X to 62:X species

that represent a substantial proportion of the TAG species in the *acc1** mutant strain are not present in the *Drosophila* TAG profile at all. In line, the large proportion of saturated TAG species (X:0) observed for the brewer's yeast is only partly reflected in the TAG profile of 1 day old *Drosophila* males. In sum, during fly development – from embryogenesis and larval development over pupariation and metamorphosis until eclosion of the adult fly – the *Drosophila* lipid profile undergoes substantial lipidome remodelling, which is also addressed in the literature [31], [69].

Our data advocates several possibilities how *Drosophila* handles food lipids, which are i) a partial breakdown of the food lipids into shorter fatty acyl chains, ii) complete breakdown of existing lipids and a major contribution of *de novo* lipogenesis or iii) a selection for distinct lipids in the gut due to intestinal lipase specificity. Partial breakdown of food lipids has been shown to occur during peroxisomal beta-oxidation of conjugated linoleic acid (18:2) in rat tissue [70] and has been demonstrated for other substrates such as eicosanoids [71] and arachidonic acid [72], however, it remains yet elusive, whether partial peroxisomal beta-oxidation occurs for every type of fatty acid or whether it occurs in *Drosophila* tissue at all. Much more likely is that *Drosophila* directly incorporates suitable fatty acids into its lipidome and breaks down other food lipids to yield energy. In addition, distinct lipids might already be omitted from food absorption in the intestine under *ad libitum* fed conditions to prevent lipotoxic consequences in the organism. Notably, 1 day old control and bmm^{1} males show very similar TAG profiles, suggesting that the Brummer lipase has little or no contribution to the fly development between the larval stage until eclosion with regard to lipid metabolism. This might not be surprising, given that during larval development, the main objective is to build up body mass rather than optimise metabolisation of available food components, however, during metamorphosis, the whole larval body plan is rewritten to become a fly, potentially also involving various lipid remodelling events.

Having seen that the Brummer lipase – or rather lack of it – seems to have little impact during fly development, we wondered whether there is a more pronounced contribution of Brummer during maturation and the onset of fly adulthood. In order to investigate this, we analysed control and bmm^{1} males 7 days after eclosion. The total TAG content of 7 days old males was almost equal for the different yeast food sources and slightly lower in comparison to 1 day old males, which goes in line with lower food intake of adult *Drosophila* compared to the food intake of the larvae. The decrease in TAG content was seen for both the control and bmm^{1} males, showing that Brummer lipase deficiency doesn't block TAG degradation entirely, as *Drosophila* is able to degrade TAG through yet uncharacterised lipases via the Akh signalling pathway [39]. As for the 1 day old *Drosophila* males, the TAG species composition for the 7 days old males is essentially the same for all the different food sources. The differences observed for the *acc1**-fed flies are entirely lost in 7 days old males. Astonishingly, the TAG acyl chain lengths show a distinct shift towards shorter acyl chains, which is much more pronounced in the control males. This shift is likely a result of dynamic degradation and synthesis of TAGs, where long chains are degraded

and shorter chains are produced, which is why it is much less distinct for the *bmm*^{1} males, as their ability to mobilise TAG is substantially impaired.

Functioning as the main storage lipid and therefore as a reservoir to provide fatty acids for membrane lipid production and to buffer excess lipid, TAGs play an important role in the organism [13], [14]. However, to ensure organelle identity and proper functioning of compartmentalisation and vesicular trafficking, it is important that an organism has functioning membrane homeostasis warranted through tight regulation of phospholipid metabolism [52], [67]. For the phospholipids PE and PC we see decreases in the total content of the control males between 1 day and 7 days, which are most pronounced in the brewer's yeast-fed flies. For the *bmm*^{1} males, the PL contents for the flies fed with the *S. cerevisiae* strains are constant and only the PL content of the brewer's yeast-fed flies decreases. This decrease is possibly a result of the different background of the brewer's yeast, however, due to the lack of information about this strain, it would be very speculative to pinpoint these findings to specific properties. Further studies should include a more in-depth analysis of the brewer's yeast, address phospholipid contents after a longer period of *Drosophila* aging and include physiological parameters like locomotor activity, fertility, fecundity and fly survival. The PE and PC compositions show almost no observable differences between the different foods and the differences we observed for the PLs of the yeast foods are almost abolished. Only the PL species containing longer acyl chains of the *acc1** mutant strain are still slightly visible in the 1 day old flies and the higher degree of unsaturation of the brewer's yeast-fed flies is seen in the 1 day and 7 days old flies. These results show the importance of maintaining membrane homeostasis. While the TAG reservoirs undergo huge changes in the form of lipid remodelling, probably in order to provide fatty acids, the membrane lipids show almost no differences for flies of different genetic backgrounds on different diets through maturation and the onset of adulthood. Between 1 day and 7 days old flies we see an increase in the degree of unsaturation of the PEs and a decrease for the PCs. This shows that the membrane compositions are *per se* not constant over time but are capable of compensating distinct changes to maintain pivotal membrane properties under certain environmental conditions. Of note, distinct cellular processes are even actively reliant on changes in membrane fluidity, curvature or electrostatics [73].

Apart from the phospholipids, which serve important functions in regards to membrane homeostasis, another important class of lipids in *Drosophila* are the DAGs, which serve as the major transport form of neutral lipids in the haemolymph [32]. For the analysis of DAGs we see high variance between the biological samples, which is not surprising given that DAG, as a transport molecule, is subject to high fluctuation and due to high turnover rates is only present in low amounts. The DAG content of 1 day old males is of no discernible difference between the different food sources. Control males contain less DAG than *bmm*^{1} males, which goes in line with the higher TAG content of these flies and likely represents a feedback reaction to the impaired

ability to hydrolyse TAGs leading to an increased *de novo* production of DAG. The DAG species composition 1 day after eclosion is similar on all food sources, which again goes in line with our observations for the TAG species composition. As transport molecule, DAG serves a similar purpose to the organism as TAG, as its main purpose is the provision of fatty acids for the membrane lipids throughout the organism. Differences that were observed for the DAG composition of the yeast foods are almost abolished in the DAG profile of 1 day old flies. Taken together, the DAG profile of freshly eclosed flies closely resembles the TAG profile. Food lipids are either selectively absorbed or broken down to shorter acyl chains, leaving the fly with lipids that are adjusted to its specific requirements.

The large differences resulting from TAG remodelling that were observed for control and *bmm*^{1} males raise the question, whether Brummer lipase deficiency shows similar behaviour for the DAGs during maturation and the onset of adulthood, as the DAGs should only be affected indirectly. Indeed, the results for the 7 days old males are quite similar for the TAGs and DAGs. The total DAG content is almost equal for the different yeast food sources and is lower compared to 1 day old control and *bmm*^{1} males. The DAG species composition shows the same characteristic shift towards shorter acyl chains, again more pronounced in the control males. This indicates that an impairment of TAG storage mobilisation has an influence on the lipid profile of the transport molecule DAG, which itself might be forced into a role where it buffers excess lipid that can no longer be incorporated into the TAG storage.

Our findings opened up the possibility that *Drosophila* selectively absorbs fatty acids of a specific scope and excretes unwanted lipids with the faeces. In order to investigate this, we analysed faeces samples of brewer's yeast-fed control and *bmm*^{1} flies. This study was conducted to i) investigate whether it is possible to detect lipids in the faeces of *Drosophila* at all, as there is currently no precedence of such an analysis and ii) to see whether intestinal lipases in *Drosophila* have a specific scope of TAGs that can be metabolised. In regards to lipid content, the faeces samples of *bmm*^{1} flies show slightly higher amounts of TAG and lower amounts of PE, PC and DAG, however, due to the sample size of n=1 for this pilot study, any assumptions regarding differences in total amounts should be viewed as speculative. The lipid compositions of the faeces samples of the control and *bmm*^{1} flies are more or less the same. Most astonishing is the TAG composition of the faeces samples, as it shows a very limited number of different species, with high amounts of 52:X and 54:X TAGs, which, in turn, only occur in little amounts in the *Drosophila* lipidome. Moreover, the faeces contain a wide distribution in regards to the TAG degree of unsaturation, which is again not resembled in the *Drosophila* lipidome. These findings strongly suggest that the intestinal lipases, one of which being the lipase Magro (*CG5932*) regulated by the *DHR96* nuclear receptor [30], might not be able to degrade TAGs with long, highly unsaturated fatty acids esterified in their glycerol backbone. Currently there are no studies addressing intestinal lipase specificity in *Drosophila*, therefore, this might be an interesting topic for future

studies. The PE and PC compositions of the faeces samples are similar to the dietary and lipidomic phospholipid compositions, which again most likely is a result of the narrow scope of physiologically required membrane lipids in eukaryotes. The DAG composition of the faeces samples shows high amounts of 34:X and 36:X species with a wide distribution of the DAG degree of unsaturation, which is congruent with the high amounts of long acyl chains found in the TAGs and therefore additionally supports the assumption that the gastric lipases in Drosophila either specifically target shorter chains for intestinal uptake or have a higher specificity for shorter chains rather than longer chains.

In conclusion, lipid dietary constraint only has minor effects on the lipidome of *Drosophila melanogaster*. The fly utilises dietary fatty acids to its needs, with an emphasis on membrane lipids that need to be in a specific scope of fatty acyl chain lengths and degree of unsaturation in order to sustain proper membrane homeostasis. The TAG and DAG reservoirs are much more flexible and buffer excessive amounts of spare lipid. During fly maturation and the onset of adulthood, the acyl chain lengths of TAG and DAG molecules shift to shorter acyl chains, probably as a way of satisfying energy demand. *Drosophila* that is impaired in its ability to hydrolyse TAG (*i.e. bmm*^{1}) [38], shows a much less pronounced shift to shorter TAG and DAG acyl chain lengths. This is most likely a result of the uptake of long fatty acyl chains and esterification into TAG in lipid droplets, which *Drosophila* is then hindered to access again from its TAG storage due to defective storage TAG mobilisation lacking the Brummer lipase. The analysis of the faeces shows that *Drosophila* excretes TAG and DAG species with long acyl chains that are highly unsaturated, which might be a result of the *Drosophila* gastric lipases being unable to degrade these lipid molecules or having a higher specificity for shorter and more saturated TAGs and DAGs, therefore only absorbing low amounts of long chain lipids.

Outlook

Our data focuses on the utilisation of dietary lipids by male *Drosophila*. Future studies might need to include female specimens, as they potentially behave differently in response to different foods due to their lipid requirements for oogenesis [12]. As our 1 day old *Drosophila* has a very different TAG profile compared to the supplied food, it would be interesting, if and during which developmental stage *Drosophila* breaks down the long chains offered. To do so, it would be interesting to examine the lipidome of *Drosophila* throughout several developmental stages (embryo, larvae, pupae). Another important matter for the future are the amounts of sterols, steryl esters and other important membrane lipids like sphingolipids in the foods, fly lipidomes and faeces. Studies show that sterols have a high influence on the development, survival and overall health of *Drosophila* [74] and disrupted sphingolipid homeostasis can lead to reproductive defects [75]. Thus, it would be interesting to examine differences in regards to these lipids and their effect on the maturation of *Drosophila* raised on different food sources. The analysis of the faeces shows that *Drosophila* excretes TAG and DAG species with long acyl chains and a high degree of unsaturation. As there is currently not much known about the gastric lipases in *Drosophila*, nor are there any studies regarding their specificity, it would be interesting to investigate this in the future, also in the context of the function of gut microbiome under dietary constraints.

Material and methods

List of chemicals and solvents

The chemicals used in this study are summarised in Table 1. The list contains chemicals used for the extraction of the lipids, the solvents of the UPLC system and the thin-layer chromatography.

Table 1: List of chemicals

Chemical	Catalogue number	Manufacturer
Ethanol (absolute for analysis)	1.00983.2500	Merck (Darmstadt, GER)
Methanol (LC-MS grade)	1.06035.2500	Merck (Darmstadt, GER)
Isopropanol (LC-MS grade)	1.02781.2500	Merck (Darmstadt, GER)
Water (LC-MS grade)	1.15333.2500	Merck (Darmstadt, GER)
Phosphoric acid	640 K3166073	Merck (Darmstadt, GER)
Methyl-tert.-butylether (MTBE; HPLC grade)	T175.1	Roth (Karlsruhe, GER)
Formic acid (HPLC grade)	4724.1	Roth (Karlsruhe, GER)
Ammonium acetate (HPLC grade)	0599-08	J.T. Baker (Center Valley, PA, USA)
Petroleum ether	CL00.1608.2500	CHEM-LAB (Zedelgem, BEL)
Diethyl ether	CL00.0405.1000	CHEM-LAB (Zedelgem, BEL)
Acetic acid	CL00.0116.2500	CHEM-LAB (Zedelgem, BEL)
Manganese(II) chloride	63543	Fluka (Buchs, CH)
Aqua bidest.		In-house distillery
Ethanol	442159	Brenntag (Essen, GER)
Sulfuric acid (95%-97%)	1.00731.1000	Merck (Darmstadt, GER)

For the UPLC system, a gradient of two solvents was used. Solvent A was methanol/water 1/1 (v/v) containing 8 µM phosphoric acid, 10mM ammonium acetate and 0.1% formic acid. Solvent B was isopropanol containing 8 µM phosphoric acid, 10mM ammonium acetate and 0.1% formic acid.

List of devices and consumables

The devices and consumables used in the experiments are summarised in Table 2. The list contains devices and consumables used for the extraction of the lipids, the measurement via UPLC-qTOF-MS and the thin-layer chromatography.

Table 2: List of devices and consumables

Device/Consumable	Catalogue number	Manufacturer
Sarstedt SafeSeal 2 ml reaction tube	72.695.500	Sarstedt (Nümbrecht, GER)
Askubal metal bead (5 mm diameter)	504942	Askubal (Korntal-Münchingen, GER)
Retsch MM 400 mixer mill	20.745.0001	Retsch (Haan, GER)
Eppendorf Thermomixer Compact 5350	5350 000.013	Eppendorf (Hamburg, GER)
Eppendorf Centrifuge 5415R	5426 000.018	Eppendorf (Hamburg, GER)
Thermo Scientific Reacti-Vap III evaporator	TS-18826	Thermo Fisher Scientific (Waltham, USA)
ACQUITY-UPLC system	186015001, 186015006, 186015028	Waters corp. (Milford, USA)
Waters ACQUITY-UPLC BEH-C18-column, 2.1 × 150 mm, 1.7 µm	186003556	Waters corp. (Milford, USA)
Phenomenex Luna® Omega 1.6 µm C18 column 50 x 2.1 mm	OOB-4742-AN	Phenomenex (Torrance, USA)
Waters SYNAPT G1 qTOF HD mass spectrometer	N/A	Waters corp. (Milford, USA)
Memmert UNB-100 oven	N/A	Memmert (Schwabach, GER)
Speed Vac	N/A	Heraeus (Düsseldorf, GER)

Yeast strains and fly lines

The yeast strains and *D. melanogaster* lines used for the experiments are summarised in Table 3.

Table 3: Yeast strains and *D. melanogaster* lines

Strain/line	Genotype	Source
BCy907c	*MATa his3Δ1 leu2Δ0 lys2Δ0 met15Δ0 ura3Δ0*	Laboratory strain (derived from sporulation of BY4743)
QKO	*MATα his3Δ1 leu2Δ0 lys2Δ0 ura3Δ0 dga1::kanMX4 lro1::kanMX4 are1::kanMX4 are2::kanMX4*	[60]
*acc1**	*MATα ACC1^{Ser1157Ala} slc4::kanMX4 his3Δ1 leu2Δ0 lys2Δ0 ura3Δ0*	Oskar Knittelfelder, 2014, PhD Thesis
Brewer's yeast	Species and genotype unknown	Gewürzmühle Brecht (Eggenstein, GER)
w^{1118}	*w^{1118}; +/+; +/+*	VDRC (Vienna, AUT) internal stock #RKF1084
bmm^{1}	*w^{1118}; +/+; bmm^{1}/TM3, Sb^{1}*	[38] internal stock #RKF1988

Sample preparation

For the food analysis, three *S. cerevisiae* strains and one commercially available yeast strain were used. The BCy907c strain serves as wild type yeast strain. The QKO mutant, which lacks

the enzymes for TAG and SE synthesis [60] and the *acc1** mutant, which has a hyperactive acetyl-CoA carboxylase, therefore producing longer fatty acids and higher amounts of TAG [64] and additionally lacking the LPAAT enzyme Slc4, are isogenic to BCy907c. The brewer's yeast, which is also a component of the standard cornmeal-based (CM) food [66] was obtained as dry yeast from "Gewürzmühle Brecht" (see above), with no further information other than that it originates from France. The BCy907, QKO mutant and *acc1** mutant are live yeasts which were cultivated in rich medium until stationary phase and harvested via centrifugation at 3000 x g for 10 minutes. The medium was discarded and the yeast cell pellet was washed twice with sterile double-distilled water to remove residual medium. The dry brewer´s yeast was suspended with sterile double-distilled water in a 1:1 ratio (i.e. 5 g yeast and 5 ml water). 100 mg of each yeast was weighed out for food lipid extraction and lipid analysis.

For the rearing experiment, control w^{1118} and isogenic bmm^{1} *flies* were used. The flies were reared at 25 °C in a 12 hour light/12 hour dark cycle with 60 % humidity. 4-5 days old flies reared on standard cornmeal-based food were put into fly cages containing agar plates with the different yeast foods, where they laid eggs until a number of approximately 100 eggs was reached. Sufficient food supply was warranted and several parameters (hatching rate, larval locomotor activity, time until pupariation, etc.) were monitored until eclosion. Batches of 5 male flies were collected 1 day and 7 days after eclosion by Dr. Harald Hofbauer, snap frozen in liquid nitrogen and stored at -20 °C for lipid extraction.

For the faeces analysis, provided by Dr. Harald Hofbauer, 400 flies of each genotype were put in a fly cage containing agar plates with brewer´s yeast as food source and were left for 24 hours to defecate in order to gain enough material for the faeces lipid extraction and lipid analysis. The cages were then cleaned out using cotton swabs and the biological material sticking to the swabs was dissolved in 1 ml PBS buffer. Before extraction, the buffer was evaporated in a Speed Vac. For blank samples, empty cages were cleaned out with cotton swaps and PBS buffer identical to cages where flies were allowed to defecate.

Lipid extraction

The lipid extractions were performed using a protocol based on the lipid extraction described by Matyash el al. [76]. The exact procedure for each type of sample is described below.

For the lipid extraction of the yeast food samples, 100 mg of wet yeast was weighed out. For the *Drosophila* lipidome analysis, five single males each were used. For the faeces analysis, the dried faeces pellet from a single cage was used. The samples were mixed with 700 µl MTBE/methanol (10/3, v/v) in 2 ml safe-seal micro tubes, disrupted with i) glass beads in a mixer mill (20 min, 30 Hz, 4 °C) for food and faeces or with ii) a metal bead in a mixer mill (3 min, 30 Hz, 4 °C) for male flies and lipids were extracted by shaking for 24 minutes on a Thermomixer at

1400 rpm and 4 °C. 200 µl water was added and samples were again incubated on a Thermomixer for 20 minutes at 1400 rpm and 4 °C. Phase separation was performed by centrifugation for 10 minutes at 16000 x g and 4 °C. The upper organic phase was collected and dried under a stream of nitrogen. The dried organic phase was dissolved in 500 µl chloroform/methanol (2/1, v/v) and dried again under a stream of nitrogen. The organic phase was then dissolved in 200 µl chloroform/methanol (2/1, v/v) and transferred to a 0.2 ml micro-inject vial, where it was dried again and prepared for LC-MS analyses.

LC-MS-analysis of lipids

The dried lipid extracts were dissolved in 150 µl (100 µl isopropanol and 50 µl chloroform/methanol (2/1, v/v)) and 10 µl of each sample was injected for analysis using UPLC-QTOF-MS. Two different UPLC methods were used for the food lipids and the fly and faeces lipids, which will be described as method A and method B, respectively. For method A, samples were separated using an AQUITY-UPLC system equipped with a Waters BEH-C18-column, 2.1 x 150 mm, 1.7 µm. The gradient started from 55 % solvent A and 45 % solvent B and reached 100 % solvent B within 32 minutes at a flow rate of 150 µl/min, with a total run time of 50 minutes [56]. For method B, samples were separated using an AQUITY-UPLC system equipped with a Phenomenex Luna® Omega C_{18} column, 2.1 x 50 mm, 1.6 µm. The gradient started from 80 % solvent A and 20 % solvent B and reached 100 % solvent B within 18 minutes at a flow rate of 300 µl/min, with a total run time of 20 minutes. A SYNAPT™ G1 qTOF HD mass spectrometer equipped with an ESI source was used for analysis in positive ionisation mode.

With the raw data, mass lists were created using the software “MassLynx V4.1 SCN639”, which was used to determine the retention time of all the lipid species found in all the samples. The mass lists used for the different samples and lipid species can be found in the appendix. With these mass lists, the data analysis was performed using the software “Lipid Data Analyzer V2.6”. The lipid species were identified by the exact mass (mass tolerance +/- 10 ppm) of the corresponding ammonium adduct ions (TAGs), protonated ions (PLs) or the combination of sodium adducts and protonated ions with water loss (DAGs) and their retention times. The retention time tolerance settings for the LDA software were +/- 0.30 minutes for the food lipids and +/- 0.15 minutes for the fly and faeces lipids [77]. The lipid data was exported to Microsoft Excel, where the total lipid content of each lipid species, as well as the relative abundance of each lipid species was calculated as percentage of the overall sum of all identified lipid species of that type (TAG, PC, PE, DAG). The detected lipid species were then grouped into their respective cumulative fatty acyl chain lengths and cumulative degree of unsaturation for comparison. As simplification and for clear depiction, the lipids of odd chain lengths were removed from the analysis.

References

[1] G. E. Allen, 'The Introduction of *Drosophila* into the Study of Heredity and Evolution: 1900-1910', *Isis*, vol. 66, no. 3, pp. 322–333, Sep. 1975, doi: 10.1086/351472.

[2] 'All Nobel Prizes in Physiology or Medicine', *NobelPrize.org*. https://www.nobelprize.org/prizes/lists/all-nobel-laureates-in-physiology-or-medicine (accessed Sep. 23, 2020).

[3] 'Six Nobel prizes – what's the fascination with the fruit fly?', *the Guardian*, Oct. 07, 2017. http://www.theguardian.com/science/2017/oct/07/fruit-fly-fascination-nobel-prizes-genetics (accessed Sep. 23, 2020).

[4] M. D. Adams *et al.*, 'The Genome Sequence of *Drosophila melanogaster*', *Science*, vol. 287, no. 5461, pp. 2185–2195, Mar. 2000, doi: 10.1126/science.287.5461.2185.

[5] M. Vidal and R. L. Cagan, '*Drosophila* models for cancer research', *Current Opinion in Genetics & Development*, vol. 16, no. 1, pp. 10–16, Feb. 2006, doi: 10.1016/j.gde.2005.12.004.

[6] A. Jeibmann and W. Paulus, '*Drosophila melanogaster* as a Model Organism of Brain Diseases', *International Journal of Molecular Sciences*, vol. 10, no. 2, Art. no. 2, Feb. 2009, doi: 10.3390/ijms10020407.

[7] Y. Apidianakis and L. G. Rahme, '*Drosophila melanogaster* as a model for human intestinal infection and pathology', *Disease Models & Mechanisms*, vol. 4, no. 1, pp. 21–30, Jan. 2011, doi: 10.1242/dmm.003970.

[8] M. Gáliková and P. Klepsatel, 'Obesity and Aging in the *Drosophila* Model', *International Journal of Molecular Sciences*, vol. 19, no. 7, Art. no. 7, Jul. 2018, doi: 10.3390/ijms19071896.

[9] B. H. Jennings, '*Drosophila* – a versatile model in biology & medicine', *Materials Today*, vol. 14, no. 5, pp. 190–195, May 2011, doi: 10.1016/S1369-7021(11)70113-4.

[10] H. Stocker and P. Gallant, 'Getting Started', in *Drosophila: Methods and Protocols*, C. Dahmann, Ed. Totowa, NJ: Humana Press, 2008, pp. 27–44.

[11] A. H. Brand and N. Perrimon, 'Targeted gene expression as a means of altering cell fates and generating dominant phenotypes', *Development*, vol. 118, no. 2, pp. 401–415, Jun. 1993.

[12] C. Heier and R. P. Kühnlein, ‘Triacylglycerol Metabolism in *Drosophila melanogaster*’, *Genetics*, vol. 210, no. 4, pp. 1163–1184, Dec. 2018, doi: 10.1534/genetics.118.301583.

[13] A. R. Thiam, R. V. Farese Jr, and T. C. Walther, ‘The biophysics and cell biology of lipid droplets’, *Nature Reviews Molecular Cell Biology*, vol. 14, no. 12, Art. no. 12, Dec. 2013, doi: 10.1038/nrm3699.

[14] R. Zechner, F. Madeo, and D. Kratky, ‘Cytosolic lipolysis and lipophagy: two sides of the same coin’, *Nature Reviews Molecular Cell Biology*, vol. 18, no. 11, Art. no. 11, Nov. 2017, doi: 10.1038/nrm.2017.76.

[15] D. Garrido, T. Rubin, M. Poidevin, B. Maroni, A. L. Rouzic, J.-P. Parvy, and J. Montagne, ‘Fatty Acid Synthase Cooperates with Glyoxalase 1 to Protect against Sugar Toxicity’, *PLOS Genetics*, vol. 11, no. 2, p. e1004995, Feb. 2015, doi: 10.1371/journal.pgen.1004995.

[16] M. A. Welte and A. P. Gould, ‘Lipid droplet functions beyond energy storage’, *Biochimica et Biophysica Acta (BBA) - Molecular and Cell Biology of Lipids*, vol. 1862, no. 10, Part B, pp. 1260–1272, Oct. 2017, doi: 10.1016/j.bbalip.2017.07.006.

[17] D. R. Nässel and J. V. Broeck, ‘Insulin/IGF signaling in *Drosophila* and other insects: factors that regulate production, release and post-release action of the insulin-like peptides’, *Cell. Mol. Life Sci.*, vol. 73, no. 2, pp. 271–290, Jan. 2016, doi: 10.1007/s00018-015-2063-3.

[18] O. Puig, M. T. Marr, M. L. Ruhf, and R. Tjian, ‘Control of cell number by *Drosophila* FOXO: downstream and feedback regulation of the insulin receptor pathway’, *Genes Dev.*, vol. 17, no. 16, pp. 2006–2020, Aug. 2003, doi: 10.1101/gad.1098703.

[19] T. Vihervaara and O. Puig, ‘dFOXO Regulates Transcription of a *Drosophila* Acid Lipase’, *Journal of Molecular Biology*, vol. 376, no. 5, pp. 1215–1223, Mar. 2008, doi: 10.1016/j.jmb.2007.12.042.

[20] G. Gäde and L. Auerswald, ‘Mode of action of neuropeptides from the adipokinetic hormone family’, *General and Comparative Endocrinology*, vol. 132, no. 1, pp. 10–20, Jun. 2003, doi: 10.1016/S0016-6480(03)00159-X.

[21] J. Baumbach, P. Hummel, I. Bickmeyer, K. M. Kowalczyk, M. Frank, K. Knorr, A. Hildebrandt, D. Riedel, H. Jäckle, and R. P. Kühnlein, ‘A *Drosophila* In Vivo Screen Identifies Store-Operated Calcium Entry as a Key Regulator of Adiposity’, *Cell Metabolism*, vol. 19, no. 2, pp. 331–343, Feb. 2014, doi: 10.1016/j.cmet.2013.12.004.

[22] T. Flatt, M.-P. Tu, and M. Tatar, ‘Hormonal pleiotropy and the juvenile hormone regulation of *Drosophila* development and life history’, *BioEssays*, vol. 27, no. 10, pp. 999–1010, 2005, doi: 10.1002/bies.20290.

[23] A. A. Baumann, J. B. Benoit, V. Michalkova, P. O. Mireji, G. M. Attardo, J. K. Moulton, T. G. Wilson, and S. Aksoy, ‘Juvenile hormone and insulin suppress lipolysis between periods of lactation during tsetse fly pregnancy’, *Molecular and Cellular Endocrinology*, vol. 372, no. 1, pp. 30–41, Jun. 2013, doi: 10.1016/j.mce.2013.02.019.

[24] P. Kang, K. Chang, Y. Liu, M. Bouska, A. Birnbaum, G. Karashchuk, R. Thakore, W. Zheng, S. Post, C. S. Brent, S. Li, M. Tatar, and H. Bai, ‘*Drosophila* Kruppel homolog 1 represses lipolysis through interaction with dFOXO’, *Scientific Reports*, vol. 7, no. 1, Art. no. 1, Nov. 2017, doi: 10.1038/s41598-017-16638-1.

[25] C. C. Schwedes and G. E. Carney, ‘Ecdysone signaling in adult *Drosophila melanogaster*’, *Journal of Insect Physiology*, vol. 58, no. 3, pp. 293–302, Mar. 2012, doi: 10.1016/j.jinsphys.2012.01.013.

[26] M. H. Sieber and A. C. Spradling, ‘Steroid Signaling Establishes a Female Metabolic State and Regulates SREBP to Control Oocyte Lipid Accumulation’, *Current Biology*, vol. 25, no. 8, pp. 993–1004, Apr. 2015, doi: 10.1016/j.cub.2015.02.019.

[27] G. E. Carney and M. Bender, ‘The *Drosophila* ecdysone receptor (EcR) Gene Is Required Maternally for Normal Oogenesis’, *Genetics*, vol. 154, no. 3, pp. 1203–1211, Mar. 2000.

[28] V. A. Francis, A. Zorzano, and A. A. Teleman, ‘dDOR Is an EcR Coactivator that Forms a Feed-Forward Loop Connecting Insulin and Ecdysone Signaling’, *Current Biology*, vol. 20, no. 20, pp. 1799–1808, Oct. 2010, doi: 10.1016/j.cub.2010.08.055.

[29] L. E. Canavoso, Z. E. Jouni, K. J. Karnas, J. E. Pennington, and M. A. Wells, ‘Fat Metabolism in Insects’, *Annual Review of Nutrition*, vol. 21, no. 1, pp. 23–46, 2001, doi: 10.1146/annurev.nutr.21.1.23.

[30] M. H. Sieber and C. S. Thummel, ‘The DHR96 Nuclear Receptor Controls Triacylglycerol Homeostasis in *Drosophila*’, *Cell Metabolism*, vol. 10, no. 6, pp. 481–490, Dec. 2009, doi: 10.1016/j.cmet.2009.10.010.

[31] M. Carvalho, J. L. Sampaio, W. Palm, M. Brankatschk, S. Eaton, and A. Shevchenko, ‘Effects of diet and development on the *Drosophila* lipidome’, *Molecular Systems Biology*, vol. 8, no. 1, p. 600, Jan. 2012, doi: 10.1038/msb.2012.29.

[32] W. Palm, J. L. Sampaio, M. Brankatschk, M. Carvalho, A. Mahmoud, A. Shevchenko, and S. Eaton, 'Lipoproteins in *Drosophila melanogaster*—Assembly, Function, and Influence on Tissue Lipid Composition', *PLOS Genetics*, vol. 8, no. 7, p. e1002828, Jul. 2012, doi: 10.1371/journal.pgen.1002828.

[33] K. Song, S. Wang, M. Mani, and A. Mani, 'Wnt signaling, de novo lipogenesis, adipogenesis and ectopic fat', *Oncotarget*, vol. 5, no. 22, pp. 11000–11003, Nov. 2014.

[34] E. Parra-Peralbo and J. Culi, '*Drosophila* Lipophorin Receptors Mediate the Uptake of Neutral Lipids in Oocytes and Imaginal Disc Cells by an Endocytosis-Independent Mechanism', *PLOS Genetics*, vol. 7, no. 2, p. e1001297, Oct. 2011, doi: 10.1371/journal.pgen.1001297.

[35] J.-P. Parvy, L. Napal, T. Rubin, M. Poidevin, L. Perrin, C. Wicker-Thomas, and J. Montagne, '*Drosophila melanogaster* Acetyl-CoA-Carboxylase Sustains a Fatty Acid–Dependent Remote Signal to Waterproof the Respiratory System', *PLOS Genetics*, vol. 8, no. 8, p. e1002925, Aug. 2012, doi: 10.1371/journal.pgen.1002925.

[36] H. Chino and L. I. Gilbert, 'Diglyceride Release from Insect Fat Body: A Possible Means of Lipid Transport', *Science*, vol. 143, no. 3604, pp. 359–361, Jan. 1964, doi: 10.1126/science.143.3604.359.

[37] E. L. Arrese and M. A. Wells, 'Adipokinetic hormone-induced lipolysis in the fat body of an insect, *Manduca sexta*: synthesis of sn-1,2-diacylglycerols.', *J. Lipid Res.*, vol. 38, no. 1, pp. 68–76, Jan. 1997.

[38] S. Grönke, A. Mildner, S. Fellert, N. Tennagels, S. Petry, G. Müller, H. Jäckle, and R. P. Kühnlein, 'Brummer lipase is an evolutionary conserved fat storage regulator in *Drosophila*', *Cell Metabolism*, vol. 1, no. 5, pp. 323–330, May 2005, doi: 10.1016/j.cmet.2005.04.003.

[39] S. Grönke, G. Müller, J. Hirsch, S. Fellert, A. Andreou, T. Haase, H. Jäckle, and R. P. Kühnlein, 'Dual Lipolytic Control of Body Fat Storage and Mobilization in *Drosophila*', *PLOS Biology*, vol. 5, no. 6, p. e137, Aug. 2007, doi: 10.1371/journal.pbio.0050137.

[40] J. Bi, Y. Xiang, H. Chen, Z. Liu, S. Grönke, R. P. Kühnlein, and X. Huang, 'Opposite and redundant roles of the two *Drosophila* perilipins in lipid mobilization', *J Cell Sci*, vol. 125, no. 15, pp. 3568–3577, Aug. 2012, doi: 10.1242/jcs.101329.

[41] S. Smith, A. Witkowski, and A. K. Joshi, 'Structural and functional organization of the animal fatty acid synthase', *Progress in Lipid Research*, vol. 42, no. 4, pp. 289–317, Jul. 2003, doi: 10.1016/S0163-7827(02)00067-X.

[42] M. C. Barber, N. T. Price, and M. T. Travers, ‘Structure and regulation of acetyl-CoA carboxylase genes of metazoa’, *Biochimica et Biophysica Acta (BBA) - Molecular and Cell Biology of Lipids*, vol. 1733, no. 1, pp. 1–28, Mar. 2005, doi: 10.1016/j.bbalip.2004.12.001.

[43] C. Wicker-Thomas, D. Garrido, G. Bontonou, L. Napal, N. Mazuras, B. Denis, T. Rubin, J.-P. Parvy, and J. Montagne, ‘Flexible origin of hydrocarbon/pheromone precursors in *Drosophila melanogaster*’, *J. Lipid Res.*, vol. 56, no. 11, pp. 2094–2101, Nov. 2015, doi: 10.1194/jlr.M060368.

[44] R. M. Bell and R. A. Coleman, ‘Enzymes of Glycerolipid Synthesis in Eukaryotes’, *Annual Review of Biochemistry*, vol. 49, no. 1, pp. 459–487, 1980, doi: 10.1146/annurev.bi.49.070180.002331.

[45] Q. Liu, R. M. P. Siloto, R. Lehner, S. J. Stone, and R. J. Weselake, ‘Acyl-CoA:diacylglycerol acyltransferase: Molecular biology, biochemistry and biotechnology’, *Progress in Lipid Research*, vol. 51, no. 4, pp. 350–377, Oct. 2012, doi: 10.1016/j.plipres.2012.06.001.

[46] H. Wang, M. V. Airola, and K. Reue, ‘How lipid droplets “TAG” along: Glycerolipid synthetic enzymes and lipid storage’, *Biochimica et Biophysica Acta (BBA) - Molecular and Cell Biology of Lipids*, vol. 1862, no. 10, Part B, pp. 1131–1145, Oct. 2017, doi: 10.1016/j.bbalip.2017.06.010.

[47] V. R. Chintapalli, J. Wang, and J. A. T. Dow, ‘Using FlyAtlas to identify better *Drosophila melanogaster* models of human disease’, *Nature Genetics*, vol. 39, no. 6, Art. no. 6, Jun. 2007, doi: 10.1038/ng2049.

[48] F. Wilfling, H. Wang, J. T. Haas, N. Krahmer, T. J. Gould, A. Uchida, J.-X. Cheng, M. Graham, R. Christiano, F. Fröhlich, X. Liu, K. K. Buhman, R. A. Coleman, J. Bewersdorf, R. V. Farese, and T. C. Walther, ‘Triacylglycerol Synthesis Enzymes Mediate Lipid Droplet Growth by Relocalizing from the ER to Lipid Droplets’, *Developmental Cell*, vol. 24, no. 4, pp. 384–399, Feb. 2013, doi: 10.1016/j.devcel.2013.01.013.

[49] M. Buszczak, X. Lu, W. A. Segraves, T. Y. Chang, and L. Cooley, ‘Mutations in the midway Gene Disrupt a *Drosophila* Acyl Coenzyme A: Diacylglycerol Acyltransferase’, *Genetics*, vol. 160, no. 4, pp. 1511–1518, Apr. 2002.

[50] D. E. Vance and J. E. Vance, *Biochemistry of Lipids, Lipoproteins and Membranes*, 4th ed. Elsevier, 2008.

[51] O. Lavrynenko, J. Rodenfels, M. Carvalho, N. A. Dye, R. Lafont, S. Eaton, and A. Shevchenko, ‘The ecdysteroidome of *Drosophila*: influence of diet and development’, *Development*, vol. 142, no. 21, pp. 3758–3768, Nov. 2015, doi: 10.1242/dev.124982.

[52] G. van Meer, D. R. Voelker, and G. W. Feigenson, ‘Membrane lipids: where they are and how they behave’, *Nature Reviews Molecular Cell Biology*, vol. 9, no. 2, Art. no. 2, Feb. 2008, doi: 10.1038/nrm2330.

[53] M. Brankatschk, T. Gutmann, O. Knittelfelder, A. Palladini, E. Prince, M. Grzybek, B. Brankatschk, A. Shevchenko, Ü. Coskun, and S. Eaton, ‘A Temperature-Dependent Switch in Feeding Preference Improves *Drosophila* Development and Survival in the Cold’, *Developmental Cell*, vol. 46, no. 6, pp. 781-793.e4, Sep. 2018, doi: 10.1016/j.devcel.2018.05.028.

[54] M. E. Swartz, ‘UPLC™: An Introduction and Review’, *Journal of Liquid Chromatography & Related Technologies*, vol. 28, no. 7–8, pp. 1253–1263, Apr. 2005, doi: 10.1081/JLC-200053046.

[55] M. Thammana, ‘A Review on High Performance Liquid Chromatography (HPLC)’, *undefined*, 2016. /paper/A-Review-on-High-Performance-Liquid-Chromatography-Thammana/ae437aeb0a2ed9ba79230ca34211a1e2253ae0e1 (accessed Sep. 08, 2020).

[56] O. L. Knittelfelder, B. P. Weberhofer, T. O. Eichmann, S. D. Kohlwein, and G. N. Rechberger, ‘A versatile ultra-high performance LC-MS method for lipid profiling’, *Journal of Chromatography B*, vol. 951–952, pp. 119–128, Mar. 2014, doi: 10.1016/j.jchromb.2014.01.011.

[57] J. B. Fenn, M. Mann, C. K. Meng, S. F. Wong, and C. M. Whitehouse, ‘Electrospray ionization for mass spectrometry of large biomolecules’, *Science*, vol. 246, no. 4926, pp. 64–71, Oct. 1989, doi: 10.1126/science.2675315.

[58] F. Lottspeich and H. Zorbas, *Bioanalytik*. Spektrum Akademischer Verlag, 1998.

[59] M. Gey, *Instrumentelle Analytik und Bioanalytik: Biosubstanzen, Trennmethoden, Strukturanalytik, Applikationen*, 3rd ed. Springer Spektrum, 2015.

[60] J. Petschnigg, H. Wolinski, D. Kolb, G. Zellnig, C. F. Kurat, K. Natter, and S. D. Kohlwein, ‘Good Fat, Essential Cellular Requirements for Triacylglycerol Synthesis to Maintain Membrane Homeostasis in Yeast’, *J. Biol. Chem.*, vol. 284, no. 45, pp. 30981–30993, Nov. 2009, doi: 10.1074/jbc.M109.024752.

[61] J. Garbarino, M. Padamsee, L. Wilcox, P. M. Oelkers, D. D’Ambrosio, K. V. Ruggles, N. Ramsey, O. Jabado, A. Turkish, and S. L. Sturley, ‘Sterol and diacylglycerol acyltransferase deficiency triggers fatty acid-mediated cell death’, *J. Biol. Chem.*, vol. 284, no. 45, pp. 30994–31005, Nov. 2009, doi: 10.1074/jbc.M109.050443.

[62] M. Hasslacher, A. S. Ivessa, F. Paltauf, and S. D. Kohlwein, ‘Acetyl-CoA carboxylase from yeast is an essential enzyme and is regulated by factors that control phospholipid metabolism.’, *J. Biol. Chem.*, vol. 268, no. 15, pp. 10946–10952, May 1993.

[63] Dr. B. E. Staveley, ‘Model Organism: *Drosophila melanogaster*’, Sep. 08, 2020. http://www.mun.ca/biology/desmid/brian/BIOL3530/DEVO_02/devo_02.html (accessed Sep. 08, 2020).

[64] H. F. Hofbauer, F. H. Schopf, H. Schleifer, O. L. Knittelfelder, B. Pieber, G. N. Rechberger, H. Wolinski, M. L. Gaspar, C. O. Kappe, J. Stadlmann, K. Mechtler, A. Zenz, K. Lohner, O. Tehlivets, S. A. Henry, and S. D. Kohlwein, ‘Regulation of Gene Expression through a Transcriptional Repressor that Senses Acyl-Chain Length in Membrane Phospholipids’, *Developmental Cell*, vol. 29, no. 6, pp. 729–739, Jun. 2014, doi: 10.1016/j.devcel.2014.04.025.

[65] C. E. Martin, C.-S. Oh, and Y. Jiang, ‘Regulation of long chain unsaturated fatty acid synthesis in yeast’, *Biochimica et Biophysica Acta (BBA) - Molecular and Cell Biology of Lipids*, vol. 1771, no. 3, pp. 271–285, Mar. 2007, doi: 10.1016/j.bbalip.2006.06.010.

[66] M. Gáliková, M. Diesner, P. Klepsatel, P. Hehlert, Y. Xu, I. Bickmeyer, R. Predel, and R. P. Kühnlein, ‘Energy Homeostasis Control in *Drosophila* Adipokinetic Hormone Mutants’, *Genetics*, vol. 201, no. 2, pp. 665–683, Oct. 2015, doi: 10.1534/genetics.115.178897.

[67] M. F. Renne and A. I. P. M. de Kroon, ‘The role of phospholipid molecular species in determining the physical properties of yeast membranes’, *FEBS Lett.*, vol. 592, no. 8, pp. 1330–1345, 2018, doi: 10.1002/1873-3468.12944.

[68] S. S. Grewal, ‘Controlling animal growth and body size - does fruit fly physiology point the way?’, *F1000 Biology Reports*, vol. 4, p. 12, 2012, doi: 10.3410/B4-12.

[69] X. L. Guan, G. Cestra, G. Shui, A. Kuhrs, R. B. Schittenhelm, E. Hafen, F. G. van der Goot, C. C. Robinett, M. Gatti, M. Gonzalez-Gaitan, and M. R. Wenk, ‘Biochemical Membrane Lipidomics during *Drosophila* Development’, *Developmental Cell*, vol. 24, no. 1, pp. 98–111, Jan. 2013, doi: 10.1016/j.devcel.2012.11.012.

[70] S. Banni, A. Petroni, M. Blasevich, G. Carta, E. Angioni, E. Murru, B. W. Day, M. P. Melis, S. Spada, and C. Ip, ‘Detection of conjugated C16 PUFAs in rat tissues as possible partial beta-oxidation products of naturally occurring conjugated linoleic acid and its metabolites’, *Biochimica et Biophysica Acta (BBA) - Molecular and Cell Biology of Lipids*, vol. 1682, no. 1, pp. 120–127, Jun. 2004, doi: 10.1016/j.bbalip.2004.03.003.

[71] J. K. Reddy and T. Hashimoto, ‘PEROXISOMAL β-OXIDATION AND PEROXISOME PROLIFERATOR–ACTIVATED RECEPTOR α: An Adaptive Metabolic System’, *Annual Review of Nutrition*, vol. 21, no. 1, pp. 193–230, 2001, doi: 10.1146/annurev.nutr.21.1.193.

[72] J. A. Gordon, S. K. Heller, T. L. Kaduce, and A. A. Spector, ‘Formation and release of a peroxisome-dependent arachidonic acid metabolite by human skin fibroblasts.’, *J. Biol. Chem.*, vol. 269, no. 6, pp. 4103–4109, Feb. 1994.

[73] J. Bigay and B. Antonny, ‘Curvature, lipid packing, and electrostatics of membrane organelles: defining cellular territories in determining specificity.’, *Dev Cell*, vol. 23, no. 5, pp. 886–895, Nov. 2012, doi: 10.1016/j.devcel.2012.10.009.

[74] J. Cooke and J. H. Sang, ‘Utilization of sterols by larvae of *Drosophila melanogaster*’, *Journal of Insect Physiology*, vol. 16, no. 5, pp. 801–812, May 1970, doi: 10.1016/0022-1910(70)90214-3.

[75] V. H. Phan, D. R. Herr, D. Panton, H. Fyrst, J. D. Saba, and G. L. Harris, ‘Disruption of sphingolipid metabolism elicits apoptosis-associated reproductive defects in *Drosophila*’, *Developmental Biology*, vol. 309, no. 2, pp. 329–341, Sep. 2007, doi: 10.1016/j.ydbio.2007.07.021.

[76] V. Matyash, G. Liebisch, T. V. Kurzchalia, A. Shevchenko, and D. Schwudke, ‘Lipid extraction by methyl-tert-butyl ether for high-throughput lipidomics’, *J. Lipid Res.*, vol. 49, no. 5, pp. 1137–1146, May 2008, doi: 10.1194/jlr.D700041-JLR200.

[77] J. Hartler, M. Trötzmüller, C. Chitraju, F. Spener, H. C. Köfeler, and G. G. Thallinger, ‘Lipid Data Analyzer: unattended identification and quantitation of lipids in LC-MS data’, *Bioinformatics*, vol. 27, no. 4, pp. 572–577, Feb. 2011, doi: 10.1093/bioinformatics/btq699.

List of figures

List of tables

Appendix

Mass lists

For the identification of the different lipid species by the software “Lipid Data Analyzer V2.6”, three different mass lists were used for the yeast foods, fly lines and faeces samples. Tables 4-15 show the mass lists for all lipid classes for the food, flies and faeces.

Table 4: Food TAGs mass list

TAG	Formula	Mass [Da]	NH_4^+ adduct [m/z]	RT [min]
TAG 34:0	C37 H70 O6	610.5172	628.5516	22.01
TAG 35:0	C38 H72 O6	624.5329	642.5672	22.84
IS TAG36:0	C39 H74 O6	638.5485	656.5829	23.62
TAG 38:0	C41 H78 O6	666.5798	684.6142	25.10
TAG 38:1	C41 H76 O6	664.5642	682.5985	24.40
TAG 40:0	C43 H82 O6	694.6111	712.6455	26.40
TAG 40:1	C43 H80 O6	692.5955	710.6298	25.28
TAG 42:0	C45 H86 O6	722.6424	740.6768	27.64
TAG 42:1	C45 H84 O6	720.6268	738.6611	26.66
TAG 42:2	C45 H82 O6	718.6111	736.6455	25.51
TAG 43:0	C46 H88 O6	736.6581	754.6924	27.90
TAG 43:1	C46 H86 O6	734.6424	752.6768	27.18
TAG 43:2	C46 H84 O6	732.6268	750.6611	26.16
TAG 44:0	C47 H90 O6	750.6737	768.7081	28.42
TAG 44:1	C47 H88 O6	748.6581	766.6924	27.77
TAG 44:2	C47 H86 O6	746.6424	764.6768	26.76
TAG 44:3	C47 H84 O6	744.6268	762.6611	25.88
IS TAG45:0	C48 H92 O6	764.6894	782.7237	29.20
TAG 45:1	C48 H90 O6	762.6737	780.7081	28.42
TAG 45:2	C48 H88 O6	760.6581	778.6924	27.31
TAG 46:0	C49 H94 O6	778.7050	796.7394	29.67
TAG 46:1	C49 H92 O6	776.6894	794.7237	28.79
TAG 46:2	C49 H90 O6	774.6737	792.7081	28.00
TAG 46:3	C49 H88 O6	772.6581	790.6924	26.89
TAG 47:0	C50 H96 O6	792.7207	810.7550	30.13
TAG 47:1	C50 H94 O6	790.7050	808.7394	29.30
TAG 47:2	C50 H92 O6	788.6894	806.7237	28.42
TAG 47:3	C50 H90 O6	786.6737	804.7081	27.49
TAG 48:0	C51 H98 O6	806.7363	824.7707	30.55
TAG 48:1	C51 H96 O6	804.7207	822.7550	29.80
TAG 48:2	C51 H94 O6	802.7050	820.7394	28.89
TAG 48:3	C51 H92 O6	800.6894	818.7237	28.01
TAG 48:4	C51 H90 O6	798.6737	816.7081	27.23
TAG 49:0	C52 H100 O6	820.7520	838.7863	31.04
TAG 49:1	C52 H98 O6	818.7363	836.7707	30.26
TAG 49:2	C52 H96 O6	816.7207	834.7550	29.38
TAG 49:3	C52 H94 O6	814.7050	832.7394	28.55
TAG 50:0	C53 H102 O6	834.7676	852.8020	31.46
TAG 50:1	C53 H100 O6	832.7520	850.7863	30.68
TAG 50:2	C53 H98 O6	830.7363	848.7707	29.90
TAG 50:3	C53 H96 O6	828.7207	846.7550	29.07
TAG 50:4	C53 H94 O6	826.7050	844.7394	28.32
IS TAG51:0	C54 H104 O6	848.7833	866.8176	31.80
TAG 51:1	C54 H102 O6	846.7676	864.8020	31.10
TAG 51:2	C54 H100 O6	844.7520	862.7863	30.32
TAG 51:3	C54 H98 O6	842.7363	860.7707	29.49
TAG 52:0	C55 H106 O6	862.7989	880.8333	32.29
TAG 52:1	C55 H104 O6	860.7833	878.8176	31.51
TAG 52:2	C55 H102 O6	858.7676	876.8020	30.81
TAG 52:3	C55 H100 O6	856.7520	874.7863	29.98
TAG 52:4	C55 H98 O6	854.7363	872.7707	29.30
TAG 53:0	C56 H108 O6	876.8146	894.8489	32.57
TAG 53:1	C56 H106 O6	874.7989	892.8333	31.93

TAG 53:2	C56 H104 O6	872.7833	890.8176	31.23
TAG 53:3	C56 H102 O6	870.7676	888.8020	30.45
TAG 54:0	C57 H110 O6	890.8302	908.8646	32.94
TAG 54:1	C57 H108 O6	888.8146	906.8489	32.29
TAG 54:2	C57 H106 O6	886.7989	904.8333	31.56
TAG 54:3	C57 H104 O6	884.7833	902.8176	30.86
TAG 54:4	C57 H102 O6	882.7676	900.8020	30.21
TAG 54:5	C57 H100 O6	880.7520	898.7863	29.56
TAG 54:6	C57 H98 O6	878.7363	896.7707	29.20
TAG 55:0	C58 H112 O6	904.8459	922.8802	33.17
TAG 55:1	C58 H110 O6	902.8302	920.8646	32.71
TAG 55:2	C58 H108 O6	900.8146	918.8489	31.98
TAG 55:3	C58 H106 O6	898.7989	916.8333	31.38
TAG 56:0	C59 H114 O6	918.8615	936.8959	33.41
TAG 56:1	C59 H112 O6	916.8459	934.8802	32.94
TAG 56:2	C59 H110 O6	914.8302	932.8646	32.34
TAG 56:3	C59 H108 O6	912.8146	930.8489	31.56
IS TAG57:0	C60 H116 O6	932.8772	950.9115	33.64
TAG 57:1	C60 H114 O6	930.8615	948.8959	33.22
TAG 57:2	C60 H112 O6	928.8459	946.8802	32.71
TAG 58:0	C61 H118 O6	946.8928	964.9272	33.82
TAG 58:1	C61 H116 O6	944.8772	962.9115	33.46
TAG 58:2	C61 H114 O6	942.8615	960.8959	33.04
TAG 58:3	C61 H112 O6	940.8459	958.8802	32.34
TAG 59:0	C62 H120 O6	960.9085	978.9428	34.00
TAG 59:1	C62 H118 O6	958.8928	976.9272	33.72
TAG 59:2	C62 H116 O6	956.8772	974.9115	33.30
TAG 59:3	C62 H114 O6	954.8615	972.8959	32.76
TAG 60:0	C63 H122 O6	974.9241	992.9585	34.13
TAG 60:1	C63 H120 O6	972.9085	990.9428	33.87
TAG 60:2	C63 H118 O6	970.8928	988.9272	33.54
TAG 60:3	C63 H116 O6	968.8772	986.9115	32.94
TAG 61:0	C64 H124 O6	988.9398	1006.9741	34.29
TAG 61:1	C64 H122 O6	986.9241	1004.9585	34.00
TAG 61:2	C64 H120 O6	984.9085	1002.9428	33.72
TAG 61:3	C64 H118 O6	982.8928	1000.9272	33.30
TAG 62:0	C65 H126 O6	1002.9554	1020.9898	34.42
TAG 62:1	C65 H124 O6	1000.9398	1018.9741	34.18
TAG 62:2	C65 H122 O6	998.9241	1016.9585	33.87
TAG 62:3	C65 H120 O6	996.9085	1014.9428	33.46
TAG 63:0	C66 H128 O6	1016.9711	1035.0054	34.55
TAG 63:1	C66 H126 O6	1014.9554	1032.9898	34.29
TAG 63:2	C66 H124 O6	1012.9398	1030.9741	34.05
TAG 64:0	C67 H130 O6	1030.9867	1049.0211	34.65
TAG 64:1	C67 H128 O6	1028.9711	1047.0054	34.47
TAG 64:2	C67 H126 O6	1026.9554	1044.9898	34.18
TAG 64:3	C67 H124 O6	1024.9398	1042.9741	33.87
TAG 65:0	C68 H132 O6	1045.0024	1063.0367	34.78
TAG 65:1	C68 H130 O6	1042.9867	1061.0211	34.55
TAG 65:2	C68 H128 O6	1040.9711	1059.0054	34.37
TAG 65:3	C68 H126 O6	1038.9554	1056.9898	34.05
TAG 66:0	C69 H134 O6	1059.0180	1077.0524	34.88
TAG 66:1	C69 H132 O6	1057.0024	1075.0367	34.70
TAG 66:2	C69 H130 O6	1054.9867	1073.0211	34.42
TAG 66:3	C69 H128 O6	1052.9711	1071.0054	34.29
TAG 68:1	C71 H136 O6	1085.0337	1103.0680	34.96
TAG 68:2	C71 H134 O6	1083.0180	1101.0524	34.70
TAG 70:1	C73 H140 O6	1113.0650	1131.0993	35.12
TAG 70:2	C73 H138 O6	1111.0493	1129.0837	34.88

Table 5: Food PE mass list

PE	**Formula**	**Mass [Da]**	**H^+ adduct [m/z]**	**RT [min]**
PE 28:0	C33 H66 O8 P1 N1	635.4526	636.4598	14.35
PE 28:1	C33 H64 O8 P1 N1	633.4369	634.4442	12.59

PE 28:2	C33 H62 O8 P1 N1	631.4213	632.4285	11.21
PE 29:1	C34 H66 O8 P1 N1	647.4526	648.4598	13.6
PE 30:1	C35 H68 O8 P1 N1	661.4682	662.4755	14.67
PE 30:2	C35 H66 O8 P1 N1	659.4526	660.4598	13.11
PE 31:1	C36 H70 O8 P1 N1	675.4839	676.4911	15.73
PE 31:2	C36 H68 O8 P1 N1	673.4682	674.4755	14.12
PE 32:1	C37 H72 O8 P1 N1	689.4995	690.5068	16.79
PE 32:2	C37 H70 O8 P1 N1	687.4839	688.4911	15.13
PE 32:3	C37 H68 O8 P1 N1	685.4682	686.4755	14.25
PE 33:1	C38 H74 O8 P1 N1	703.5152	704.5224	17.76
PE 33:2	C38 H72 O8 P1 N1	701.4995	702.5068	16.14
PE 33:3	C38 H70 O8 P1 N1	699.4839	700.4911	14.02
PE 33:4	C38 H68 O8 P1 N1	697.4682	698.4755	12.17
IS PE34:0	C39 H78 O8 P1 N1	719.5465	720.5537	20.17
PE 34:1	C39 H76 O8 P1 N1	717.5308	718.5381	18.69
PE 34:2	C39 H74 O8 P1 N1	715.5152	716.5224	17.16
PE 34:3	C39 H72 O8 P1 N1	713.4995	714.5068	15.78
PE 35:1	C40 H78 O8 P1 N1	731.5465	732.5537	19.60
PE 36:0	C41 H82 O8 P1 N1	747.5778	748.5850	21.83
PE 36:1	C41 H80 O8 P1 N1	745.5621	746.5694	20.48
PE 36:2	C41 H78 O8 P1 N1	743.5465	744.5537	19.00
PE 36:3	C41 H76 O8 P1 N1	741.5308	742.5381	17.75

Table 6: Food PC mass list

PC	**Formula**	**Mass [Da]**	**H^+ adduct [m/z]**	**RT [min]**
PC 26:0	C34 H68 O8 P1 N1	649.4682	650.4755	11.81
PC 26:1	C34 H66 O8 P1 N1	647.4526	648.4598	10.10
PC 26:2	C34 H64 O8 P1 N1	645.4369	646.4442	8.95
PC 27:0	C35 H70 O8 P1 N1	663.4839	664.4911	12.87
PC 27:1	C35 H68 O8 P1 N1	661.4682	662.4755	11.11
PC 28:0	C36 H72 O8 P1 N1	677.4995	678.5068	14.02
PC 28:1	C36 H70 O8 P1 N1	675.4839	676.4911	12.22
PC 28:2	C36 H68 O8 P1 N1	673.4682	674.4755	10.88
PC 29:1	C37 H72 O8 P1 N1	689.4995	690.5068	13.29
PC 30:0	C38 H76 O8 P1 N1	705.5308	706.5381	16.01
PC 30:1	C38 H74 O8 P1 N1	703.5152	704.5224	14.35
PC 30:2	C38 H72 O8 P1 N1	701.4995	702.5068	12.77
PC 31:1	C39 H76 O8 P1 N1	717.5308	718.5381	15.44
PC 31:2	C39 H74 O8 P1 N1	715.5152	716.5224	13.78
PC 32:0	C40 H80 O8 P1 N1	733.5621	734.5694	18.04
PC 32:1	C40 H78 O8 P1 N1	731.5465	732.5537	16.43
PC 32:2	C40 H76 O8 P1 N1	729.5308	730.5381	14.77
PC 32:3	C40 H74 O8 P1 N1	727.5152	728.5224	13.47
PC 33:1	C41 H80 O8 P1 N1	745.5621	746.5694	17.44
PC 33:2	C41 H78 O8 P1 N1	743.5465	744.5537	15.78
IS PC34:0	C42 H84 O8 P1 N1	761.5934	762.6007	19.88
PC 34:1	C42 H82 O8 P1 N1	759.5778	760.5850	18.40
PC 34:2	C42 H80 O8 P1 N1	757.5621	758.5694	16.79
PC 34:3	C42 H78 O8 P1 N1	755.5465	756.5537	15.50
PC 35:0	C43 H86 O8 P1 N1	775.6091	776.6163	20.71
PC 35:1	C43 H84 O8 P1 N1	773.5934	774.6007	19.28
PC 35:2	C43 H82 O8 P1 N1	771.5778	772.5850	17.75
PC 36:0	C44 H88 O8 P1 N1	789.6247	790.6320	21.54
PC 36:1	C44 H86 O8 P1 N1	787.6091	788.6163	20.17
PC 36:2	C44 H84 O8 P1 N1	785.5934	786.6007	18.69
PC 36:3	C44 H82 O8 P1 N1	783.5778	784.5850	17.39
PC 37:0	C45 H90 O8 P1 N1	803.6404	804.6476	22.32
PC 37:1	C45 H88 O8 P1 N1	801.6247	802.6320	20.53
PC 37:2	C45 H86 O8 P1 N1	799.6091	800.6163	19.52
IS PC38:0	C46 H92 O8 P1 N1	817.6560	818.6633	23.07
PC 38:1	C46 H90 O8 P1 N1	815.6404	816.6476	21.83
PC 38:2	C46 H88 O8 P1 N1	813.6247	814.6320	20.35
PC 39:0	C47 H94 O8 P1 N1	831.6717	832.6789	23.75
PC 40:0	C48 H96 O8 P1 N1	845.6873	846.6946	24.40

PC 40:1	C48 H94 O8 P1 N1	843.6717	844.6789	23.34
PC 40:2	C48 H92 O8 P1 N1	841.6560	842.6633	21.91
PC 41:1	C49 H96 O8 P1 N1	857.6873	858.6946	24.09

Table 7: Food DAG mass list

DAG	Formula	Mass [Da]	Na^+ adduct [m/z]	H^+-H_2O adduct [m/z]	RT [min]
IS DAG28:0	C31 H60 O5	512.4441	535.4339	495.4413	17.57
DAG 28:1	C31 H58 O5	510.4284	533.4182	493.4257	15.78
DAG 30:0	C33 H64 O5	540.4754	563.4652	523.4726	19.52
DAG 30:1	C33 H62 O5	538.4597	561.4495	521.4570	17.94
DAG 30:2	C33 H60 O5	536.4441	559.4339	519.4413	16.33
DAG 32:0	C35 H68 O5	568.5067	591.4965	551.5039	21.31
DAG 32:1	C35 H66 O5	566.4910	589.4808	549.4883	19.83
DAG 32:2	C35 H64 O5	564.4754	587.4652	547.4726	18.27
DAG 34:0	C37 H72 O5	596.5380	619.5278	579.5352	23.02
DAG 34:1	C37 H70 O5	594.5223	617.5121	577.5196	21.60
DAG 34:2	C37 H68 O5	592.5067	615.4965	575.5039	20.12
DAG 36:1	C39 H74 O5	622.5536	645.5434	605.5509	23.20
DAG 36:2	C39 H72 O5	620.5380	643.5278	603.5352	21.83
DAG 38:2	C41 H76 O5	648.5693	671.5591	631.5665	23.34

Table 8: Fly TAG mass list

TAG	Formula	Mass [Da]	NH_4^+ adduct [m/z]	RT [min]
TAG 34:0	C37 H70 O6	610.5172	628.5516	11.88
TAG 34:1	C37 H68 O6	608.5016	626.5359	11.29
TAG 35:0	C38 H72 O6	624.5329	642.5672	12.29
IS TAG36:0	C39 H74 O6	638.5485	656.5829	12.67
TAG 36:1	C39 H72 O6	636.5329	654.5672	12.12
TAG 36:2	C39 H70 O6	634.5172	652.5516	11.53
TAG 37:0	C40 H76 O6	652.5642	670.5985	13.04
TAG 37:1	C40 H74 O6	650.5485	668.5829	12.55
TAG 38:0	C41 H78 O6	666.5798	684.6142	13.40
TAG 38:1	C41 H76 O6	664.5642	682.5985	12.93
TAG 39:0	C42 H80 O6	680.5955	698.6298	13.74
TAG 39:1	C42 H78 O6	678.5798	696.6142	13.28
TAG 40:0	C43 H82 O6	694.6111	712.6455	14.09
TAG 40:1	C43 H80 O6	692.5955	710.6298	13.62
TAG 40:2	C43 H78 O6	690.5798	708.6142	13.26
TAG 40:3	C43 H76 O6	688.5642	706.5985	12.95
TAG 41:0	C44 H84 O6	708.6268	726.6611	14.37
TAG 41:1	C44 H82 O6	706.6111	724.6455	13.95
TAG 41:2	C44 H80 O6	704.5955	722.6298	13.62
TAG 42:0	C45 H86 O6	722.6424	740.6768	14.70
TAG 42:1	C45 H84 O6	720.6268	738.6611	14.28
TAG 42:2	C45 H82 O6	718.6111	736.6455	13.84
TAG 42:3	C45 H80 O6	716.5955	734.6298	13.58
TAG 42:4	C45 H78 O6	714.5798	732.6142	13.30
TAG 43:0	C46 H88 O6	736.6581	754.6924	14.98
TAG 43:1	C46 H86 O6	734.6424	752.6768	14.55
TAG 43:2	C46 H84 O6	732.6268	750.6611	14.13
TAG 43:3	C46 H82 O6	730.6111	748.6455	13.72
TAG 44:0	C47 H90 O6	750.6737	768.7081	15.26
TAG 44:1	C47 H88 O6	748.6581	766.6924	14.85
TAG 44:2	C47 H86 O6	746.6424	764.6768	14.43
TAG 44:3	C47 H84 O6	744.6268	762.6611	14.02
IS TAG45:0	C48 H92 O6	764.6894	782.7237	15.53
TAG 45:1	C48 H90 O6	762.6737	780.7081	15.11
TAG 45:2	C48 H88 O6	760.6581	778.6924	14.74

TAG 45:3	C48 H86 O6	758.6424	776.6768	14.35
TAG 45:4	C48 H84 O6	756.6268	774.6611	13.89
TAG 46:0	C49 H94 O6	778.7050	796.7394	15.81
TAG 46:1	C49 H92 O6	776.6894	794.7237	15.40
TAG 46:2	C49 H90 O6	774.6737	792.7081	15.00
TAG 46:3	C49 H88 O6	772.6581	790.6924	14.63
TAG 47:0	C50 H96 O6	792.7207	810.7550	16.03
TAG 47:1	C50 H94 O6	790.7050	808.7394	15.66
TAG 47:2	C50 H92 O6	788.6894	806.7237	15.29
TAG 47:3	C50 H90 O6	786.6737	804.7081	14.89
TAG 47:4	C50 H88 O6	784.6581	802.6924	14.50
TAG 48:0	C51 H98 O6	806.7363	824.7707	16.27
TAG 48:1	C51 H96 O6	804.7207	822.7550	15.92
TAG 48:2	C51 H94 O6	802.7050	820.7394	15.55
TAG 48:3	C51 H92 O6	800.6894	818.7237	15.16
TAG 48:4	C51 H90 O6	798.6737	816.7081	14.76
TAG 49:0	C52 H100 O6	820.7520	838.7863	16.53
TAG 49:1	C52 H98 O6	818.7363	836.7707	16.19
TAG 49:2	C52 H96 O6	816.7207	834.7550	15.79
TAG 49:3	C52 H94 O6	814.7050	832.7394	15.44
TAG 49:4	C52 H92 O6	812.6894	830.7237	15.09
TAG 49:5	C52 H90 O6	810.6737	828.7081	14.65
TAG 50:0	C53 H102 O6	834.7676	852.8020	16.75
TAG 50:1	C53 H100 O6	832.7520	850.7863	16.40
TAG 50:2	C53 H98 O6	830.7363	848.7707	16.05
TAG 50:3	C53 H96 O6	828.7207	846.7550	15.70
TAG 50:4	C53 H94 O6	826.7050	844.7394	15.36
IS TAG51:0	C54 H104 O6	848.7833	866.8176	16.95
TAG 51:1	C54 H102 O6	846.7676	864.8020	16.64
TAG 51:2	C54 H100 O6	844.7520	862.7863	16.29
TAG 51:3	C54 H98 O6	842.7363	860.7707	15.94
TAG 51:4	C54 H96 O6	840.7207	858.7550	15.64
TAG 51:5	C54 H94 O6	838.7050	856.7394	15.24
TAG 52:0	C55 H106 O6	862.7989	880.8333	17.19
TAG 52:1	C55 H104 O6	860.7833	878.8176	16.86
TAG 52:2	C55 H102 O6	858.7676	876.8020	16.53
TAG 52:3	C55 H100 O6	856.7520	874.7863	16.19
TAG 52:4	C55 H98 O6	854.7363	872.7707	15.85
TAG 53:0	C56 H108 O6	876.8146	894.8489	17.36
TAG 53:1	C56 H106 O6	874.7989	892.8333	17.08
TAG 53:2	C56 H104 O6	872.7833	890.8176	16.75
TAG 53:3	C56 H102 O6	870.7676	888.8020	16.40
TAG 54:0	C57 H110 O6	890.8302	908.8646	17.56
TAG 54:1	C57 H108 O6	888.8146	906.8489	17.28
TAG 54:2	C57 H106 O6	886.7989	904.8333	16.95
TAG 54:3	C57 H104 O6	884.7833	902.8176	16.64
TAG 54:4	C57 H102 O6	882.7676	900.8020	16.34
TAG 54:5	C57 H100 O6	880.7520	898.7863	16.01
TAG 55:0	C58 H112 O6	904.8459	922.8802	17.71
TAG 55:1	C58 H110 O6	902.8302	920.8646	17.47
TAG 55:2	C58 H108 O6	900.8146	918.8489	17.17
TAG 56:0	C59 H114 O6	918.8615	936.8959	17.85
TAG 56:1	C59 H112 O6	916.8459	934.8802	17.65
TAG 56:2	C59 H110 O6	914.8302	932.8646	17.36
TAG 56:3	C59 H108 O6	912.8146	930.8489	17.04
IS TAG57:0	C60 H116 O6	932.8772	950.9115	17.95
TAG 57:1	C60 H114 O6	930.8615	948.8959	17.83
TAG 57:2	C60 H112 O6	928.8459	946.8802	17.58
TAG 58:0	C61 H118 O6	946.8928	964.9272	18.04
TAG 58:1	C61 H116 O6	944.8772	962.9115	17.89
TAG 58:2	C61 H114 O6	942.8615	960.8959	17.71

TAG 58:3	C61 H112 O6	940.8459	958.8802	17.43
TAG 59:0	C62 H120 O6	960.9085	978.9428	18.11
TAG 60:0	C63 H122 O6	974.9241	992.9585	18.17
TAG 60:1	C63 H120 O6	972.9085	990.9428	18.09
TAG 60:2	C63 H118 O6	970.8928	988.9272	17.91
TAG 60:3	C63 H116 O6	968.8772	986.9115	17.75
TAG 62:1	C65 H124 O6	1000.9398	1018.9741	18.22
TAG 62:2	C65 H122 O6	998.9241	1016.9585	18.11

Table 9: Fly PE mass list

PE	**Formula**	**Mass [Da]**	**H^+ adduct [m/z]**	**RT [min]**
PE 30:0	C35 H70 O8 P1 N1	663.4839	664.4911	8.32
PE 30:1	C35 H68 O8 P1 N1	661.4682	662.4755	7.75
PE 31:1	C36 H70 O8 P1 N1	675.4839	676.4911	8.16
PE 32:1	C37 H72 O8 P1 N1	689.4995	690.5068	8.54
PE 32:2	C37 H70 O8 P1 N1	687.4839	688.4911	7.99
PE 33:1	C38 H74 O8 P1 N1	703.5152	704.5224	9.03
PE 33:2	C38 H72 O8 P1 N1	701.4995	702.5068	8.42
IS PE34:0	C39 H78 O8 P1 N1	719.5465	720.5537	10.04
PE 34:1	C39 H76 O8 P1 N1	717.5308	718.5381	9.45
PE 34:2	C39 H74 O8 P1 N1	715.5152	716.5224	8.84
PE 34:3	C39 H72 O8 P1 N1	713.4995	714.5068	8.32
PE 35:1	C40 H78 O8 P1 N1	731.5465	732.5537	9.89
PE 35:2	C40 H76 O8 P1 N1	729.5308	730.5381	9.25
PE 36:1	C41 H80 O8 P1 N1	745.5621	746.5694	10.30
PE 36:2	C41 H78 O8 P1 N1	743.5465	744.5537	9.69
PE 36:3	C41 H76 O8 P1 N1	741.5308	742.5381	9.17
PE 36:4	C41 H74 O8 P1 N1	739.5152	740.5224	8.71
PE 38:1	C43 H84 O8 P1 N1	773.5934	774.6007	11.13
PE 38:2	C43 H82 O8 P1 N1	771.5778	772.5850	10.48
PE 40:1	C45 H88 O8 P1 N1	801.6247	802.6320	11.90

Table 10: Fly PC mass list

PC	**Formula**	**Mass [Da]**	**H^+ adduct [m/z]**	**RT [min]**
PC 26:0	C34 H68 O8 P1 N1	649.4682	650.4755	6.56
PC 28:0	C36 H72 O8 P1 N1	677.4995	678.5068	7.39
PC 28:1	C36 H70 O8 P1 N1	675.4839	676.4911	6.85
PC 28:2	C36 H68 O8 P1 N1	673.4682	674.4755	6.48
PC 29:0	C37 H74 O8 P1 N1	691.5152	692.5224	7.79
PC 29:1	C37 H72 O8 P1 N1	689.4995	690.5068	7.22
PC 30:0	C38 H76 O8 P1 N1	705.5308	706.5381	8.20
PC 30:1	C38 H74 O8 P1 N1	703.5152	704.5224	7.61
PC 30:2	C38 H72 O8 P1 N1	701.4995	702.5068	7.18
PC 31:0	C39 H78 O8 P1 N1	719.5465	720.5537	8.54
PC 31:1	C39 H76 O8 P1 N1	717.5308	718.5381	8.05
PC 31:2	C39 H74 O8 P1 N1	715.5152	716.5224	7.46
PC 32:0	C40 H80 O8 P1 N1	733.5621	734.5694	9.10
PC 32:1	C40 H78 O8 P1 N1	731.5465	732.5537	8.47
PC 32:2	C40 H76 O8 P1 N1	729.5308	730.5381	7.90
PC 33:1	C41 H80 O8 P1 N1	745.5621	746.5694	8.90
PC 33:2	C41 H78 O8 P1 N1	743.5465	744.5537	8.29
IS PC34:0	C42 H84 O8 P1 N1	761.5934	762.6007	9.93
PC 34:1	C42 H82 O8 P1 N1	759.5778	760.5850	9.30
PC 34:2	C42 H80 O8 P1 N1	757.5621	758.5694	8.73
PC 34:3	C42 H78 O8 P1 N1	755.5465	756.5537	8.20
PC 34:4	C42 H76 O8 P1 N1	753.5308	754.5381	7.73
PC 35:1	C43 H84 O8 P1 N1	773.5934	774.6007	9.78
PC 35:2	C43 H82 O8 P1 N1	771.5778	772.5850	9.15
PC 36:0	C44 H88 O8 P1 N1	789.6247	790.6320	10.79
PC 36:1	C44 H86 O8 P1 N1	787.6091	788.6163	10.22
PC 36:2	C44 H84 O8 P1 N1	785.5934	786.6007	9.58

PC 36:3	C44 H82 O8 P1 N1	783.5778	784.5850	9.08
PC 36:4	C44 H80 O8 P1 N1	781.5621	782.5694	8.54
IS PC38:0	C46 H92 O8 P1 N1	817.6560	818.6633	11.57

Table 11: Fly DAG mass list

DAG	Formula	Mass [Da]	Na^+ adduct [m/z]	H^+-H_2O adduct [m/z]	RT [min]
DAG 24:0	C27 H52 O5	456.3815	479.3713	439.3787	7.39
DAG 26:0	C29 H56 O5	484.4128	507.4026	467.4100	8.32
DAG 26:1	C29 H54 O5	482.3971	505.3869	465.3944	7.73
IS DAG28:0	C31 H60 O5	512.4441	535.4339	495.4413	9.41
DAG 28:1	C31 H58 O5	510.4284	533.4182	493.4257	8.58
DAG 30:0	C33 H64 O5	540.4754	563.4652	523.4726	10.20
DAG 30:1	C33 H62 O5	538.4597	561.4495	521.4570	9.52
DAG 30:2	C33 H60 O5	536.4441	559.4339	519.4413	8.93
DAG 32:1	C35 H66 O5	566.4910	589.4808	549.4883	10.39
DAG 32:2	C35 H64 O5	564.4754	587.4652	547.4726	9.76
DAG 34:1	C37 H70 O5	594.5223	617.5121	577.5196	11.27
DAG 34:2	C37 H68 O5	592.5067	615.4965	575.5039	10.65
DAG 36:1	C39 H74 O5	622.5536	645.5434	605.5509	12.10
DAG 36:2	C39 H72 O5	620.5380	643.5278	603.5352	11.53

Table 12: Faeces TAG mass list

TAG	Formula	Mass [Da]	NH_4^+ adduct [m/z]	RT [min]
TAG 38:0	C41 H78 O6	666.5798	684.6142	13.62
TAG 40:0	C43 H82 O6	694.6111	712.6455	14.28
TAG 40:1	C43 H80 O6	692.5955	710.6298	13.95
TAG 40:2	C43 H78 O6	690.5798	708.6142	13.45
TAG 41:0	C44 H84 O6	708.6268	726.6611	14.45
TAG 41:1	C44 H82 O6	706.6111	724.6455	13.87
TAG 42:0	C45 H86 O6	722.6424	740.6768	14.92
TAG 42:1	C45 H84 O6	720.6268	738.6611	14.50
TAG 43:0	C46 H88 O6	736.6581	754.6924	15.14
TAG 43:1	C46 H86 O6	734.6424	752.6768	14.81
TAG 44:0	C47 H90 O6	750.6737	768.7081	15.46
TAG 44:1	C47 H88 O6	748.6581	766.6924	15.09
TAG 44:2	C47 H86 O6	746.6424	764.6768	14.70
TAG 44:3	C47 H84 O6	744.6268	762.6611	14.28
TAG 45:0	C48 H92 O6	764.6894	782.7237	15.68
TAG 45:1	C48 H90 O6	762.6737	780.7081	15.38
TAG 45:2	C48 H88 O6	760.6581	778.6924	14.96
TAG 46:0	C49 H94 O6	778.7050	796.7394	15.97
TAG 46:1	C49 H92 O6	776.6894	794.7237	15.66
TAG 46:2	C49 H90 O6	774.6737	792.7081	15.31
TAG 46:3	C49 H88 O6	772.6581	790.6924	14.96
TAG 46:4	C49 H86 O6	770.6424	788.6768	14.63
TAG 47:0	C50 H96 O6	792.7207	810.7550	16.21
TAG 47:1	C50 H94 O6	790.7050	808.7394	15.92
TAG 47:2	C50 H92 O6	788.6894	806.7237	15.55
TAG 47:3	C50 H90 O6	786.6737	804.7081	15.22
TAG 48:0	C51 H98 O6	806.7363	824.7707	16.45
TAG 48:1	C51 H96 O6	804.7207	822.7550	16.12
TAG 48:2	C51 H94 O6	802.7050	820.7394	15.79
TAG 48:3	C51 H92 O6	800.6894	818.7237	15.51
TAG 48:4	C51 H90 O6	798.6737	816.7081	15.02
TAG 49:0	C52 H100 O6	820.7520	838.7863	16.66
TAG 49:1	C52 H98 O6	818.7363	836.7707	16.31
TAG 49:2	C52 H96 O6	816.7207	834.7550	16.01
TAG 49:3	C52 H94 O6	814.7050	832.7394	15.75
TAG 50:0	C53 H102 O6	834.7676	852.8020	16.90
TAG 50:1	C53 H100 O6	832.7520	850.7863	16.58
TAG 50:2	C53 H98 O6	830.7363	848.7707	16.27
TAG 50:3	C53 H96 O6	828.7207	846.7550	15.94

TAG 50:4	C53 H94 O6	826.7050	844.7394	15.55
TAG 50:5	C53 H92 O6	824.6894	842.7237	15.22
TAG 51:0	C54 H104 O6	848.7833	866.8176	17.10
TAG 51:1	C54 H102 O6	846.7676	864.8020	16.80
TAG 51:2	C54 H100 O6	844.7520	862.7863	16.47
TAG 51:3	C54 H98 O6	842.7363	860.7707	16.21
TAG 51:4	C54 H96 O6	840.7207	858.7550	15.79
TAG 52:0	C55 H106 O6	862.7989	880.8333	17.34
TAG 52:1	C55 H104 O6	860.7833	878.8176	17.02
TAG 52:2	C55 H102 O6	858.7676	876.8020	16.68
TAG 52:3	C55 H100 O6	856.7520	874.7863	16.38
TAG 52:4	C55 H98 O6	854.7363	872.7707	16.05
TAG 52:5	C55 H96 O6	852.7207	870.7550	15.75
TAG 52:6	C55 H94 O6	850.7050	868.7394	15.42
TAG 53:0	C56 H108 O6	876.8146	894.8489	17.49
TAG 53:1	C56 H106 O6	874.7989	892.8333	17.23
TAG 53:2	C56 H104 O6	872.7833	890.8176	16.92
TAG 53:3	C56 H102 O6	870.7676	888.8020	16.62
TAG 53:4	C56 H100 O6	868.7520	886.7863	16.29
TAG 53:5	C56 H98 O6	866.7363	884.7707	15.94
TAG 54:0	C57 H110 O6	890.8302	908.8646	17.69
TAG 54:1	C57 H108 O6	888.8146	906.8489	17.41
TAG 54:2	C57 H106 O6	886.7989	904.8333	17.12
TAG 54:3	C57 H104 O6	884.7833	902.8176	16.82
TAG 54:4	C57 H102 O6	882.7676	900.8020	16.51
TAG 54:5	C57 H100 O6	880.7520	898.7863	16.19
TAG 54:6	C57 H98 O6	878.7363	896.7707	15.85
TAG 54:7	C57 H96 O6	876.7207	894.7550	15.53
TAG 54:8	C57 H94 O6	874.7050	892.7394	15.20
TAG 54:9	C57 H92 O6	872.6894	890.7237	14.87
TAG 55:0	C58 H112 O6	904.8459	922.8802	17.83
TAG 55:1	C58 H110 O6	902.8302	920.8646	17.65
TAG 55:2	C58 H108 O6	900.8146	918.8489	17.34
TAG 55:3	C58 H106 O6	898.7989	916.8333	17.04
TAG 56:0	C59 H114 O6	918.8615	936.8959	17.93
TAG 56:1	C59 H112 O6	916.8459	934.8802	17.75
TAG 56:2	C59 H110 O6	914.8302	932.8646	17.54
TAG 56:3	C59 H108 O6	912.8146	930.8489	17.23
TAG 56:4	C59 H106 O6	910.7989	928.8333	17.00
TAG 56:5	C59 H104 O6	908.7833	926.8176	16.64
TAG 56:6	C59 H102 O6	906.7676	924.8020	16.31
TAG 57:0	C60 H116 O6	932.8772	950.9115	18.00
TAG 57:1	C60 H114 O6	930.8615	948.8959	17.89
TAG 57:2	C60 H112 O6	928.8459	946.8802	17.71
TAG 58:0	C61 H118 O6	946.8928	964.9272	18.09
TAG 58:1	C61 H116 O6	944.8772	962.9115	17.97
TAG 58:2	C61 H114 O6	942.8615	960.8959	17.85
TAG 58:3	C61 H112 O6	940.8459	958.8802	17.54
TAG 58:4	C61 H110 O6	938.8302	956.8646	17.39
TAG 58:5	C61 H108 O6	936.8146	954.8489	17.12
TAG 59:0	C62 H120 O6	960.9085	978.9428	18.15
TAG 59:1	C62 H118 O6	958.8928	976.9272	18.04
TAG 59:2	C62 H116 O6	956.8772	974.9115	17.95
TAG 59:3	C62 H114 O6	954.8615	972.8959	17.78
TAG 60:0	C63 H122 O6	974.9241	992.9585	18.19
TAG 60:1	C63 H120 O6	972.9085	990.9428	18.13
TAG 60:2	C63 H118 O6	970.8928	988.9272	18.02
TAG 60:3	C63 H116 O6	968.8772	986.9115	17.89
TAG 60:4	C63 H114 O6	966.8615	984.8959	17.75
TAG 60:5	C63 H112 O6	964.8459	982.8802	17.54
TAG 61:1	C64 H122 O6	986.9241	1004.9585	18.19
TAG 61:2	C64 H120 O6	984.9085	1002.9428	18.09
TAG 62:0	C65 H126 O6	1002.9554	1020.9898	18.32
TAG 62:1	C65 H124 O6	1000.9398	1018.9741	18.24
TAG 62:2	C65 H122 O6	998.9241	1016.9585	18.15
TAG 62:3	C65 H120 O6	996.9085	1014.9428	18.09
TAG 62:4	C65 H118 O6	994.8928	1012.9272	17.95

Table 13: Faeces PE mass list

PE	Formula	Mass [Da]	H^+ adduct [m/z]	RT [min]
PE 32:1	C37 H72 O8 P1 N1	689.4995	690.5068	8.82
PE 32:2	C37 H70 O8 P1 N1	687.4839	688.4911	8.20
PE 34:1	C39 H76 O8 P1 N1	717.5308	718.5381	9.67
PE 34:2	C39 H74 O8 P1 N1	715.5152	716.5224	9.12
PE 36:1	C41 H80 O8 P1 N1	745.5621	746.5694	10.50
PE 36:2	C41 H78 O8 P1 N1	743.5465	744.5537	9.96
PE 36:3	C41 H76 O8 P1 N1	741.5308	742.5381	9.37
PE 36:4	C41 H74 O8 P1 N1	739.5152	740.5224	8.82
PE 38:1	C43 H84 O8 P1 N1	773.5934	774.6007	11.35
PE 38:2	C43 H82 O8 P1 N1	771.5778	772.5850	10.85

Table 14: Faeces PC mass list

PC	Formula	Mass [Da]	H^+ adduct [m/z]	RT [min]
PC 30:1	C38 H74 O8 P1 N1	703.5152	704.5224	7.88
PC 32:1	C40 H78 O8 P1 N1	731.5465	732.5537	8.73
PC 32:2	C40 H76 O8 P1 N1	729.5308	730.5381	8.10
PC 33:1	C41 H80 O8 P1 N1	745.5621	746.5694	9.15
PC 33:2	C41 H78 O8 P1 N1	743.5465	744.5537	8.54
PC 34:0	C42 H84 O8 P1 N1	761.5934	762.6007	10.22
PC 34:1	C42 H82 O8 P1 N1	759.5778	760.5850	9.58
PC 34:2	C42 H80 O8 P1 N1	757.5621	758.5694	8.99
PC 34:3	C42 H78 O8 P1 N1	755.5465	756.5537	8.49
PC 35:1	C43 H84 O8 P1 N1	773.5934	774.6007	10.00
PC 35:2	C43 H82 O8 P1 N1	771.5778	772.5850	9.43
PC 36:1	C44 H86 O8 P1 N1	787.6091	788.6163	10.44
PC 36:2	C44 H84 O8 P1 N1	785.5934	786.6007	9.82
PC 36:3	C44 H82 O8 P1 N1	783.5778	784.5850	9.30
PC 36:4	C44 H80 O8 P1 N1	781.5621	782.5694	8.73
PC 36:5	C44 H78 O8 P1 N1	779.5465	780.5537	8.25

Table 15: Faeces DAG mass list

DAG	Formula	Mass [Da]	Na^+ adduct [m/z]	H^+-H_2O adduct [m/z]	RT [min]
DAG 26:0	C29 H56 O5	484.4128	507.4026	467.4100	8.75
DAG 26:1	C29 H54 O5	482.3971	505.3869	465.3944	8.07
DAG 28:0	C31 H60 O5	512.4441	535.4339	495.4413	9.71
DAG 32:1	C35 H66 O5	566.4910	589.4808	549.4883	10.79
DAG 34:0	C37 H72 O5	596.5380	619.5278	579.5352	12.25
DAG 34:1	C37 H70 O5	594.5223	617.5121	577.5196	11.68
DAG 34:2	C37 H68 O5	592.5067	615.4965	575.5039	11.01
DAG 36:1	C39 H74 O5	622.5536	645.5434	605.5509	12.31
DAG 36:2	C39 H72 O5	620.5380	643.5278	603.5352	11.86
DAG 36:3	C39 H70 O5	618.5223	641.5121	601.5196	11.37
DAG 36:4	C39 H68 O5	616.5067	639.4965	599.5039	10.81